LM RADAR REFLECTIVITY SIMULATION*

Final Report - Contract NAS 9-7828

By

H. S. Hayre, R. F. Chia, and
J. Valerdi

TR-69-3

Wave Propagation Laboratory
Department of Electrical Engineering

UNIVERSITY OF HOUSTON

Cullen College of Engineering
3801 Cullen Boulevard
Houston, Texas 77004

*This work is sponsored by NASA - Manned Spacecraft Center, under Contract NAS 9-7828.

TABLE OF CONTENTS

LIST OF FIGURES

FIGURE PAGE

FIGURE PAGE

LIST OF TABLES

ACKNOWLEDGMENTS

The Wave Propagation Laboratories, Department of Electrical Engineering, Cullen College of Engineering, University of Houston, are sincerely thankful to NASA Manned Spacecraft Center and the SESD Division for sponsoring this research work. The continuous cooperation and expediting of usual needs by the NASA Manned Spacecraft Center Monitor, Mr. Douglas LaPoint, was most appreciated by the principal investigator. It is hoped that our talent and experience in simulation of radar problems be utilized by NASA on a continuing basis in the future.

ABSTRACT

An ultrasonic simulation of the radar reflectivity from LM radar was carried out for the LM lunar landing sites P-II-6 and 8 at 10, 20, 30 and 40 K ft. altitude for angles of incidence varying from zero to 50 degrees, as well as for Hummocks area (White Sands Missile Range) at zero and twenty degree angles of incidence at altitudes of 200 ft. to 1,000 ft. in 100 ft. intervals. The resulting radar cross-section with plus and minus are standard deviation values and were obtained by refering the data to a flat plate data at 10 K ft. for lunar surface models and to another flat plate at 1,000 ft. altitude for Hummocks area. The scale factor for Hummocks area was 500, and that for P-II-6 and 8 lunar landing sites was 6,850. In both cases wavelength reduced heights were used to model surface heights. The small scale random surface undulations were obtained from general information available on it. The final results in both cases verify our previous theoretical and experimental work in that the means may vary as much as ± 1.5 db from a smooth reflectivity curve and that the plus and minus sigma values of the reflectivity may vary asymmetrically as much as ± 7 db depending on the altitude. The spread is small at high altitudes and large at small altitudes. For instance, 3 db at 10 K and 0 degree incidence angle for lunar surface to -8 db at 200 ft. for Hummocks area (WSMR).

The ultrasonic simulation of radar reflectivity and its other statistics is easy, fast and inexpensive, and furthermore allows laboratory controlled conditions for all types of design studies.

CHAPTER I

LUNAR MODEL LOW ALTITUDE REFLECTIVITY

One of the major objectives of this research was to simulate the LM radar reflectivity at zero to fifty degree angles of incidence from the surface normal for altitudes varying from ten thousand to forty thousand feet for the site P-II-6 and 8 model, and to obtain the RCS as well as the variance at each angle of incidence. Furthermore, this data was to be compared with theoretically and otherwise expected results and smoothed for LM applications.

Lunar Model

The lunar landing sites P-II-6 and 8, A and B model consisted of 4' x 12' surface with the top 2' x 12' representing P-II-6, and the bottom half representing P-II-8. This model was constructed for use in reflectivity studies for altitudes between 3.4 and 25 thousand feet, employing a distance scale factor of 6850. In other words, the laboratory distances corresponding to 10, 20, 30, and 40 K feet were 17.5, 35, 52.5, and 70 inches. This site model is shown in Figure A-1. The central portion of the illuminated area in this model is essentially free of any major craters, rills and mountains, except for a ridge of P-II-6 AB-1 terminating on the center line, whereas the outer fringes consist of a few end sections of ridges of P-II-6 AB-1 in approximately fifty feet of the length of the target, and a few small craters in the remaining upper and lower regions. The surface area was relatively smooth and yet there were the usual lunar type lava rock/boulder distribution in this region. This would imply that the radar cross-section must then be high near zero angle of incidence as compared to the values at other angles.

In the near vertical incidence case, the region covered by the radar illuminated for 12^{o} beamwidth at forty thousand feet is approximately 14" wide and this covers a little less than nearly one third the width of the total 48" wide simulated model surface. The outer extremities are marked by a dotted line. The transducer set was tilted forward along the path length in order to obtain various angles of incidence, and therefore the RCS at all angles pertain to the region within the outer extremities discussed above.

The basis of this lunar landing site model was covered under a previous years' report, TR-68-17; also, the final report on NAS 9-6760, dated October, 1968. This work being a continuation of the same contract for the second year does not therefore contain a repetition of the details of this model. It may be sufficient though, to add that P-II-6 and 8 refer to two probable lunar landing sites numbered 6 and 8, and their surface data was obtained from Orbitor II mission high and low resolution cameras. Furthermore, it is also essential to include a word about the small scale roughness on this lunar surface model. The small scale lunar roughness was obtained by piecing the following types of information on the same:

a) Surveyor mission closeup photographs of the lunar surface,

b) Considerable lunar surface modeling experience by us,

c) Boulder theory regarding lunar surface makeup, and

d) Small scale roughness measure based on crater-rills-boulder size and spatial distribution.

<u>Experimental Setup and Data Format</u>

The two sections 4' x 6' each of these lunar surface models, are mounted in a vertical frame as discussed in detail in Chapter III, and the transmit-receive transducer package is so oriented and located as to yield the desired angle of incidence as well as the altitude. Then the transducer package is allowed to traverse the entire length of the target at a fixed velocity. Further details of all of the data recording are also given in Chapter III. This data is then normalized in terms of the flat plat reference data obtained by placing a flat plat at the location of the target in order to obtain decible figures.

The final data is in the form of varying dc level representing and is recorded both on a Sanborn paper recorder and on a fm channel of a Precision magnetic tape recorder whose detailed specifications are also included in Chapter III. Both of these forms of this data were supplied to NASA Manned Spacecraft Center, even though the contractual provisions requiredthe University of Houston to supply only the magnetic tape recordings only. The calibration procedure for the magnetic tape and the general experimental procedures are also given in Chapter III. A complete chapter later on describes methods of data analysis, which was carried out to supply NASA Manned Spacecraft Center with rapid results because of deadlines on the Apollo LM radar checkout, etc. A summary of all such magnetic tape recordings is given in Table A-4, and all of the paper recordings for different altitudes and angles of incidence varying from zero to fifty degrees from the outward average surface normal in Figs. A-4 through A-13. In the case of 10 K ft. altitude, the angle of incidence was varied in steps of five degrees, whereas in all other cases ten degree incremental steps were used.

All this work was carried out employing a 1.0 megacycle/sec sine wave signal, and all the subsystems were capable of handling signals bandwidths of at least 10-20 kc, thus assuring of no distortion of any information bearing signal forms. The 400 EL HP voltmeter dc output response had a slow response of few milliseconds but that did not effect the results because the Sanborn paper tape recorder tied to its output has a frequency response of approximately dc-sixty cycles, and it was the average signal which was the desired output of this experiment.

CHAPTER II

HUMMOCK SITE (WSMR) RADAR REFLECTIVITY

NASA Manned Spacecraft Center had flown the LM radar in a helicopter over the Hummock site at angles of incidence of zero and twenty degrees at various altitudes and it was desired by NASA that:

A. A laboratory model be built for Hummock site

B. LM velocity radar reflectivity simulation be made at the following altitudes for both zero and twenty degree angles of incidence:

200', 300', 400', 500', 600', 700', 800', 900', 1000'

Surface Modeling

In this case a set of terrain profiles A, B, D and E shown in Fig.A-15 and a top view of typical surface features with their horizontal and vertical dimensions in the form of contours shown in Fig.A-14 were provided to the University of Houston, Wave Propagation Laboratories. The terrain profiles were read, and wavelength-reduced in order to determine their model heights as shown in Table A-3 because for zero and twenty degree angles of incidence, the shadow effects for the surface of Hummock site are negligible for all practical purposes, as there are few sharp changes in terrain profile. The surface is basically flat with a superposition of rounded mounds of sand.

The area under consideration is approximately 50 thousand feet long and 533 feet wide, and the maximum length of a model being limited to 12 feet, it was decided to model both horizontal x and y dimensions of this area by scaling it down by a factor of 500. Thus the two 4' x 6' model sections were used to constitute the surface with only the central 10 feet length being used for this purpose. Although the transducer simulating the LM radar was to be moved along the center of this model area, the beamwidth and percent area illuminated considerations dictated that the modeled surface extend well beyond the area for which details were provided in order to eliminate edge effect on the backscattered energy. It was therefore decided to extend the basic surface features of the typical central strip to the surrounding areas in the same random fashion.

The scaled down random shaped contours were reproduced on the model surface 1/4" aluminum plate with a planemeter. The basic surface was generated by using epoxy adhesive with very fine sand of size M200 (.074 mm). The flat shaped mounds were created by piling layer after layer or in a lump sum fashion depending on their relative altitude. These were continuous piles and are not to be confused with a layered structure as such. The sharp edges were then smoothed.

The theoretical and experimental justification for ultrasonic simulation of radar return from randomly rough surfaces is given in detail later on in Chapter IV. Again in this work 1.0 inch diameter lead zirconate disc transducers mounted at the end of a cyclinderical housing were employed using 1.0 megacycle continuous wave signal. The remaining details of the experimental data taking are almost identical to that for the lunar surface except that the altitude scale factor for this model was 500.

The method of mounting the target and the transmit-receive transducer package was such that data at 100 feet altitude could not be taken, and this limitation is only temporary and shall be rectified for future work. The experimental data was taken for altitudes corresponding to actual heights of 200 through 1000 feet in 100 foot increments. The angles of incident of zero and twenty degrees were specified by NASA - MSC, because of the need for comparison of the results of this data with full-scale LM radar data taken at WSMR using a helicopter.

The full length of target for each run at each altitude and angle of incidence was believed to be sufficiently large in as far the number of independent samples taken the beamwidth of the transmit-receive transducer package as it transverses the terrain model at a fixed x-axis velocity υ_x in inches per second as specified by a linear relation between the voltage applied V to the x-axis motor controller $\upsilon_x = 0.075V - 0.125$. A setting of V = 25 volts was used to obtain the approximate velocity as given by the above equation. It was made sure during each run that the x-motor controller voltage V was maintained constant, as it was the case in the lunar experiment. This resulted in approximately the same length of data as was obtained in actual full-scale experiment at WSMR.

The parallax error was expected at very low altitudes in the vicinity of 400 feet or below this height, and the details of the said correction are discussed in later chapters. The final results are referred to a single reference flat plate for convenience and can easily be made to represent a normalized simulated radar cross section if all the curves were refered to as zero db value at the lowest altitude. The altitude and angle of incidence variation are further discussed under

CHAPTER III

GENERAL EXPERIMENTAL SYSTEM OPERATION

Mechanical Set-Up

Definition of Experiment

The experiment itself will determine the different runs that will be required and based on that information we obtain:

a) The speed of motion desired of X motor in ips

b) The fixed positions of the Y carriage in inches

c) The angle of the transducer with respect to the 0° reference, which is perpendicular to the target

d) The time duration of a run will be in functions of the velocity of the carriage (v) in motion and the distance to cover (Δx) ,

i.e.

$$\Delta t = \frac{\Delta x}{v}$$

Calibration

The calibration is done either using a twin 6' x 4' flat aluminum plate as a target and the dynamic runs are made at the different Y positions in order to get the reference levels, namely at altitudes corresponding to the 10k, 20k, 30k, and 40k feet altitude. The angle of the transducers should be kept at 0°.

Target Mounting

Two 6' x 4' sections of simulated sand targets are fixed on a 13' x 4' aluminum frame with a center angle iron (as illustrated) with eight "C" clamps, one on each corner of the targets or eight bolts. The frame is loosened and reswung from the vertical to the horizontal position by removing the locking bolts which are located at the base of each tower. The frame itself is hinged in order to allow this motion.

Back View of Targets

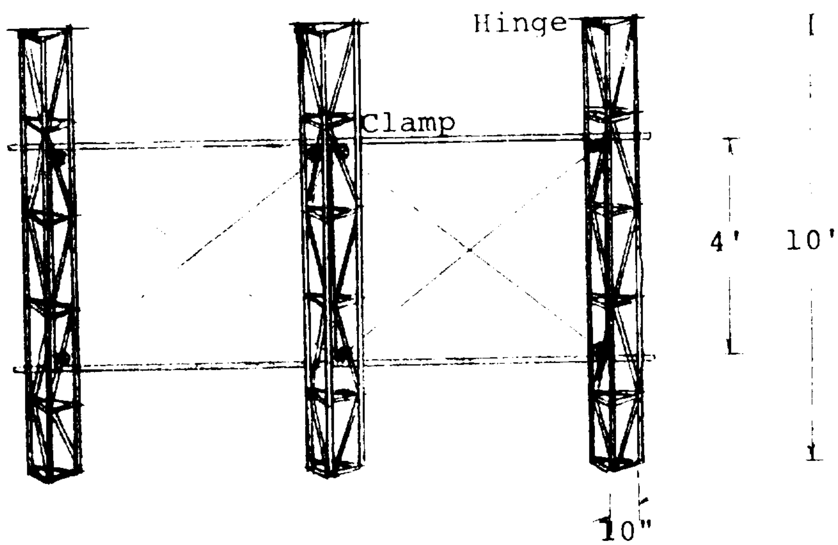

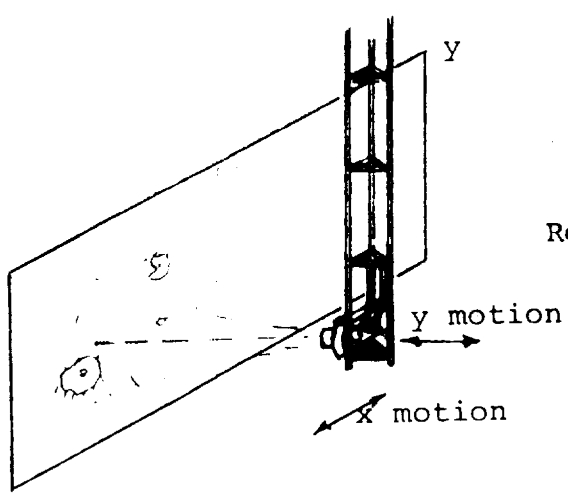

Reference:	25" 7/16	
	10k	42" 15/16
	20k	60" 2/16
	30k	77"10/16
	40k	95" 7/16

Dynamic Runs

For a dynamic run the following steps are followed:

a) Set the dc voltage applied to the X motor controller at an appropriate level for the desired horizontal velocity.

b) Set the X- and Y-static position of the carriage before starting the experiment.

c) Set the angle of the transmit-receive transducers set with respect to the vertical incidence reference zero - previously fixed.

d) Establish the absolute stationarity the water mass in the tank by allowing 30 minutes after shutting off the water filter and by ascertaining the stationarity of the transducer tower by mechanical and electrical means.

e) Record all signal levels (see calibration chart): HP voltmeter detector scale, and its DC output level.

f) Start the paper and magnetic tape recorders first and after five seconds initiate the dynamic run of the X carriage and record the output signal level.

g) Maintain constant DC voltage at the X motor controller.

Percent Accuracies

For all the readings, the various x- and y-positions of the carriage are accurate to within an 1/32 of an inch and the angle settings are accurate to within 1/4 of a degree. Since the X carriage motion was the most important dynamical part of the runs, its uniform displacement was closely watched in order to obtain a constant velocity and its repeatability was absolute as supported by its run in opposite directions.

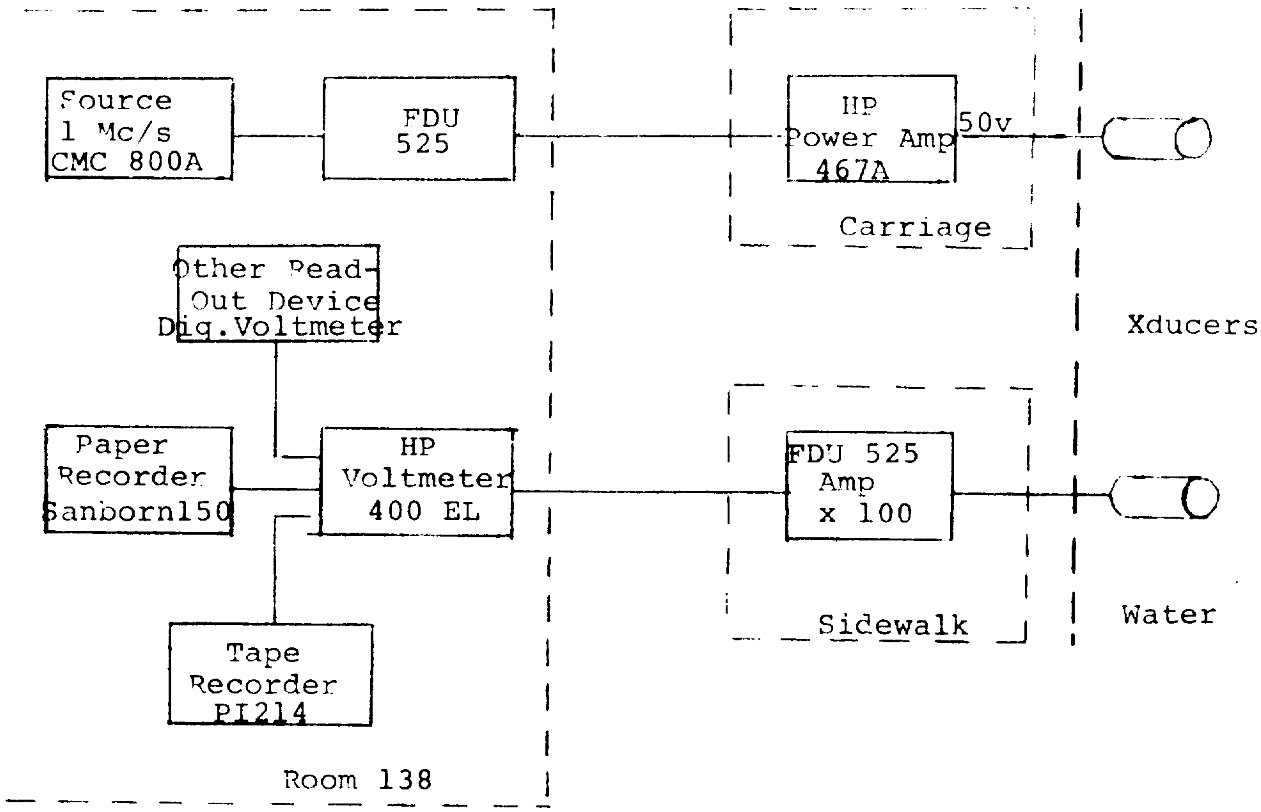

Fig. 3-0. Electrical Instrumentation

Experimental System

The LM radars were simulated by transmit-receive transducers mounted in appropriate LM orientation and the mechanical limitations of the movement of the entire package made it necessary to utilize the altimeter transmit-receive transducers for various angles of incidence settings from zero to fifty degrees. Again the present system was limited to a maximum of 50° swing, but this is being rectified to allow a complete $\pm 90^{\circ}$ swing for future work.

Incidentally, in the LM data it was not deemed critical to go to beyond 50° as the drop in RCS is significantly high as discussed later.

The basic voltage source for one megacycle/second was the CMC counter, whose output was fed into the Tracor Frequency Distribution unit, Model 525, in order to drive approximately 200 feet of 93-ohm coaxial cable to the top of our 20 foot diameter, 25 foot high water tank, where the approximately two volt RMS signal was supplied to a HP Power Amplifier Model 467A , whose output was nearly 60 volts peak to peak. This high voltage was used to drive the transmit transducer located at the end of another approximately 10 feet of 93-ohm cable. The receiver transducer produces an output of 0.1 to few hundred millivolts depending on the distance from the target as well as the nature of the target surface. This received signal forms the input to another high gain Tracor Frequency Distribution unit, Model 525, located approximately 30 feet away for amplification and driving the 200 feet of coaxial cable back to the instrumentation room at the bottom of the tank.

This signal varies from approximately 100 millivolts to 10 volts peak to peak, and is fed into HP Model 400 EL Voltmeter-Amplitude Detector, as well as a digital voltmeter for monitoring purposes. The dc output of the 400 EL voltmeter-detector is linearly proportional to the amplitude of the input sine wave at 1 mcs, as shown by data in Table 3-2 and Fig.3-1,2,3. Therefore it is then recorded on Sanborn paper recorder as well as the PI-214 magnetic tape recorder. The magnetic tape recording was done using FM channel along with a direct-record voice channel in order to provide supplemental information on each run. A complete system diagram is shown in Fig. 3-0 and a summary of the basic specifications of each of the units involved are given in Table 3-1.

Both the magnetic tape recordings and paper tape recordings were sent to Lockheed Electronics Company personnel working for NASA Manned Spacecraft Center, SESD Division, EE6 Branch, for reduction and analysis by them.

Calibration

In each run it was ascertained that the pure sine wave form of the 1 mcs signal at each point of the entire system except at the dc input of the HP voltmeter-detector 400 EL was maintained. A typical record form is shown in Fig. 3-4. Anytime this check resulted in any distortion of the signal, new power amplifier setting was used to boost the transmitted signal in order to maintain a sine wave signal well above the receiver as well as to maintain the driving voltage at a fairly constant level.

TABLE 3-1

SUB-SYSTEM SPECIFICATIONS

1. 1 mc Continuous Wave Source CMC 800A/803/833 Crystal Osc.
   Stability: Aging less than ± 3 parts in 10^9/24 hrs.
   Temperature less than ± 2 parts in $10^{10}/C^o$
   Line voltage (± 10%) less than ± 5 parts in 10^{10}
2. 525 - Frequency Distribution Unit - Line Driver (Tracor)
   Input Voltage - 0.5 to 5 V
   Input Impedance 1K ohm
   Output Voltage - Minimum 2.8 V pp at the end of 300
   Thermal Noise - 100 db below 1 V
   Cross-Talk - 50 db below signal feet of RF58/Ω coax to
   50 ohm load
3. HP 467A - Power Amplifier
   Gain 0 - 10
   Output Capability ± 20 V pp at 0.5 amp peak
   Frequency Response ± 1.0% from DC to 100 Kc
   ± 10% from DC to 1 mc
   Distortion - less than 0.01% at 1 Kc
   1.0% at 100 Kc
   3.0% at 1 mc
   Input Impednace - 50K ohms slanted by 100 pts.
   Output Impedance - 5 Milliohms in series with 1 h
   Ripple and Noise - Less than 5 mv pp.
   Capacitive Load Instability - 0.01 μf or less does not cause
   instability
4. 525 - Frequency Distribution Unit - High Gain (Tracor) Line Driver
   Minimum Input - Greater than 0.1 mv (equiv. input noise level
   = 0.05 mv)
   Gain - 1000
   Bandwidth (± 3 db pts) - 400 cps to 1.1 mc.
   Others - Same as in (2) above

TABLE 3-1 (CONT'D)

5. HP 400 EL Voltmeter/Detector (RMS Voltmeter)
   DC Output (full scale) = 1.0 volt for each scale
   DC Output proportional to percentage of meter deflection
   Accuracy of Reading ± 2% at 1.0 mc
   Scales: 0.001, 0.01, 0.1, 0.3, 1.0, 3.0, 10, 30, 100, 300 volts
   Linearity of DC output vs. AC input beyond full scale deflection (see Fig.)
6. Sanborn Model 150 Paper Recorder - 4 channels
   Paper Speeds - mm/sec - 0.25, 0.5, 1, 2.5, 5, 10, 25, 50, 100
   Sensitivities - volts/cm - 0.1, 0.2, 0.5, 1.0, 2, 5, 10, 20, 50, 100
   Time Marker
7. P-I 214 - Magnetic Tape Recorder
   FM Channels 108 Kcs ± 40%
   1, 3, 5, 7, 9, 11 - Min Rec. Level
   Calibrated for ±2 volts
   Direct Record Channels - 2, 4, 6, 8, 10, 12
     Voice Recorded on Channel 12
     Min. Record Level
     Speed Used - High - 60 IPS

Prior to any experimental run a flat aluminum plate was positioned at the location of the target surface and one or all of the experimental altitudes were selected in order to obtain an absolute vertical incidence (zero angle) as well as the corresponding reference signal. This reference signal was later used to obtain decible values for each run or corresponding altitude run as the case may be. The Branson transducers used in this work were 1.0 inch discs mounted in a waterproof cylindrical housing and are made of lead zirconate. The efficiency and directivity of the basic unmasked transmitter-receiver transducers are identical and thus do not bias the data in any way because the same set is used to obtain flat plate data used for referencing all the received signals. These transducers are rather insensitive to input voltage levels of less than 20 v p+p and respond more or less linearly for higher driving voltages. Incidentally, it was decided to maintain a constant driving voltage in order to avoid any corrections in data due to different input signal levels.

TABLE 3-2

400 EL - VOLTMETER - DETECTOR RESPONSE CALIBRATION

Digital VM Input	3.0 Scale	1.0 Scale	0.3 Scale	0.1 Scale	0.03
3.0					
2.8					
2.6					
2.4	2.38/0.747*	2.41			
2.2	2.1/0.657	2.087	3.980		
2.0	1.9/0.595	1.898	3.881		
1.8	1.7/0.537	1.710	3.794		
1.6	1.5/0.478	1.523	3.684		
1.4	1.32/0.419	1.335	3.536		
1.2	1.12/0.360	1.148	3.311		
1.0	0.95/0.300	0.96/0.957*	2.981		
0.8	0.239	0.77/0.765	2.470		
0.6	0.178	0.57/0.571	1.811	3.842	
0.4	0.117	0.375/.377	1.196	3.377	
0.3	0.086	0.215/.278	.28/0.886*	2.819	
0.25	0.071	0.229	.23/0.730	2.319	
0.20	0.055	0.180	.18/0.573	1.820	
0.15	0.041	0.133	.135/0.425	1.350	
0.10	0.027	0.090	.09/0.289	.092/0.919*	
0.05	0.015	0.052	0.171	.055/0.546	
0.04	0.012	0.042	0.136	.043/0.435	
0.03	0.009	0.030	0.100	.032/0.321	
0.02	0.005	0.019	0.065	0.209	0.021/0.
0.01	0.002	0.010	0.032	0.104	0.010/0.

FIG. 3-1 400 EL VOLTMETER-DETECTOR RESPONSE

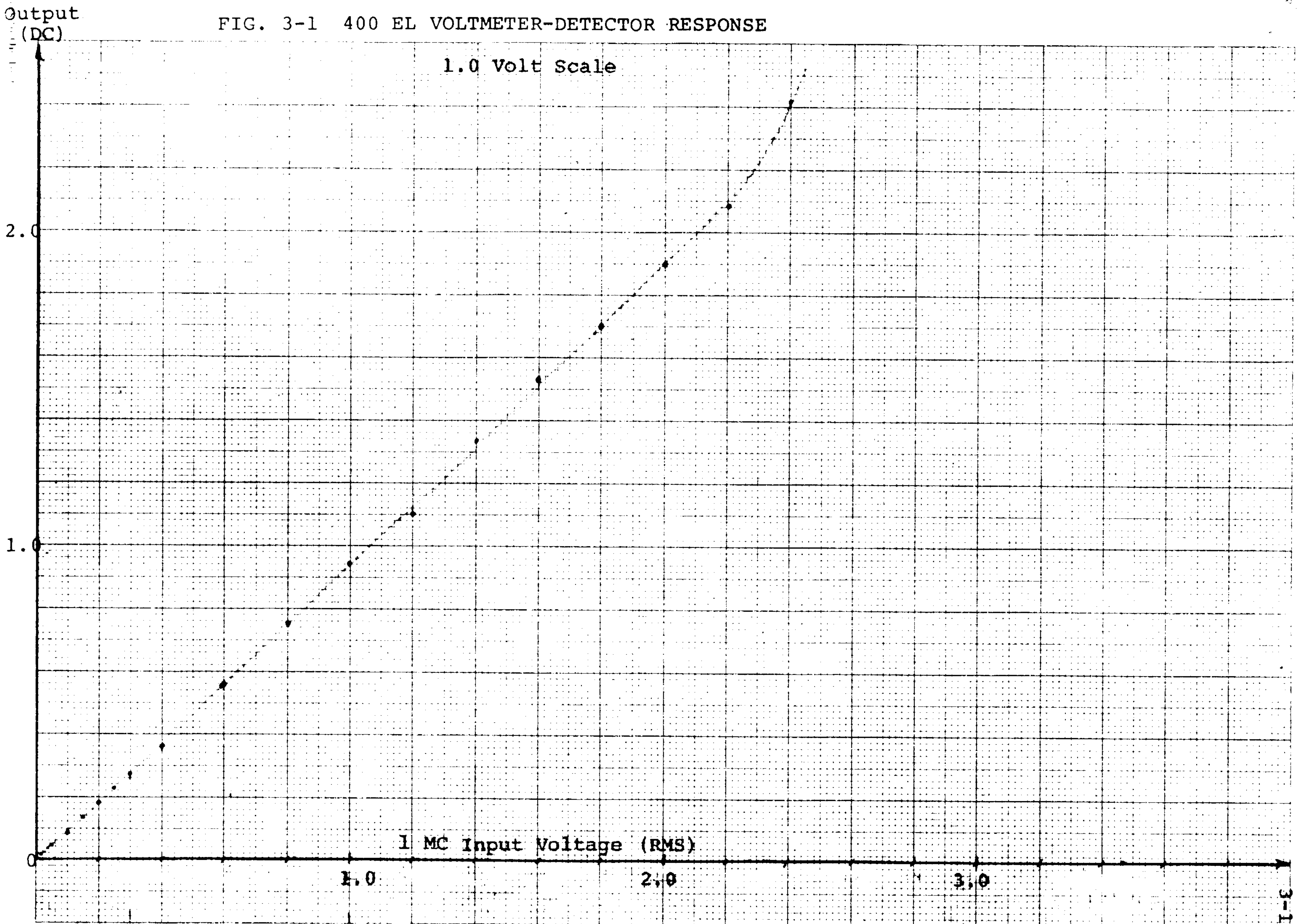

FIG. 3-2. 400 EL VOLTMETER-DETECTOR RESPONSE

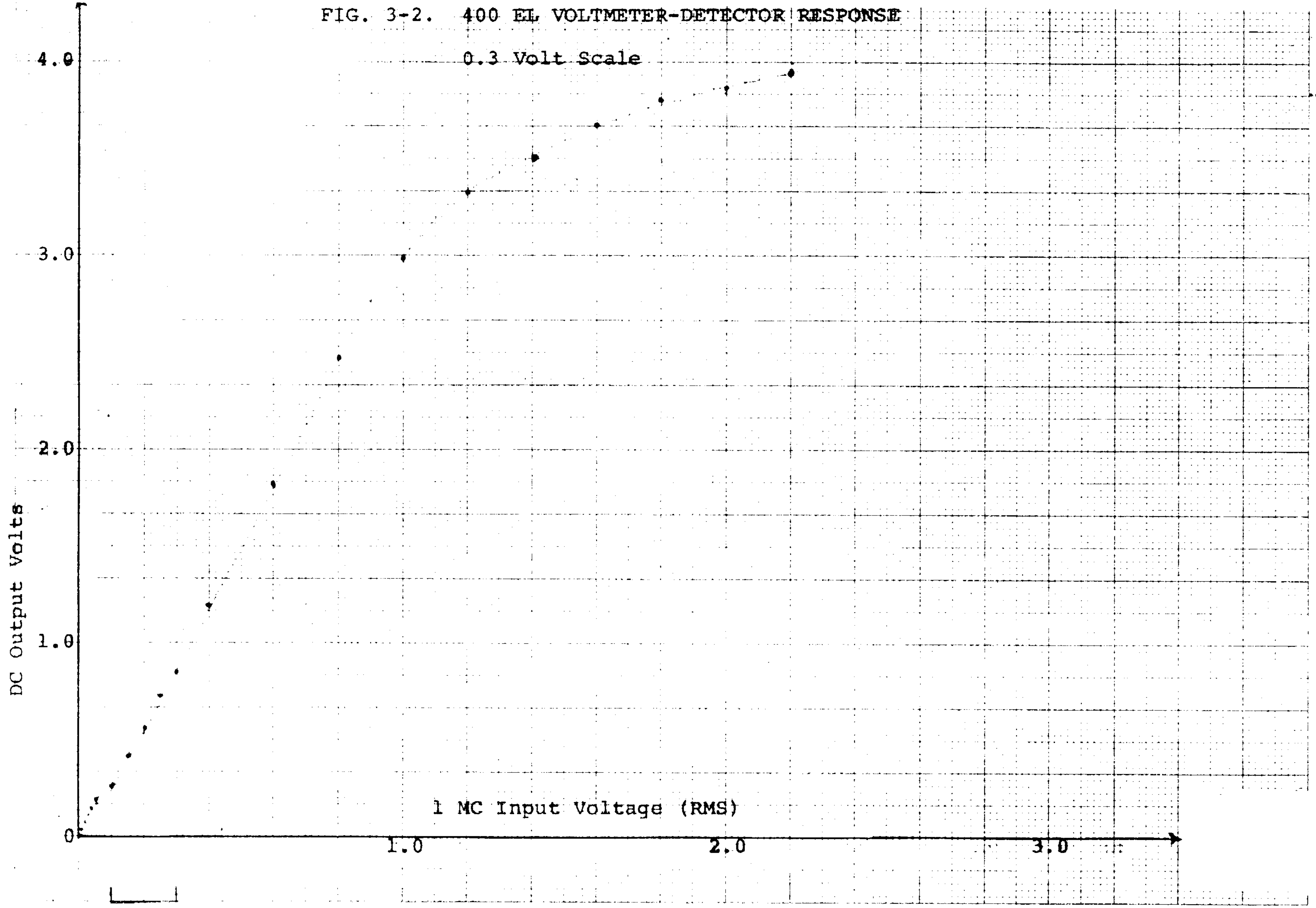

FIG. 3-3. 400 EL VOLTMETER-DETECTOR RESPONSE

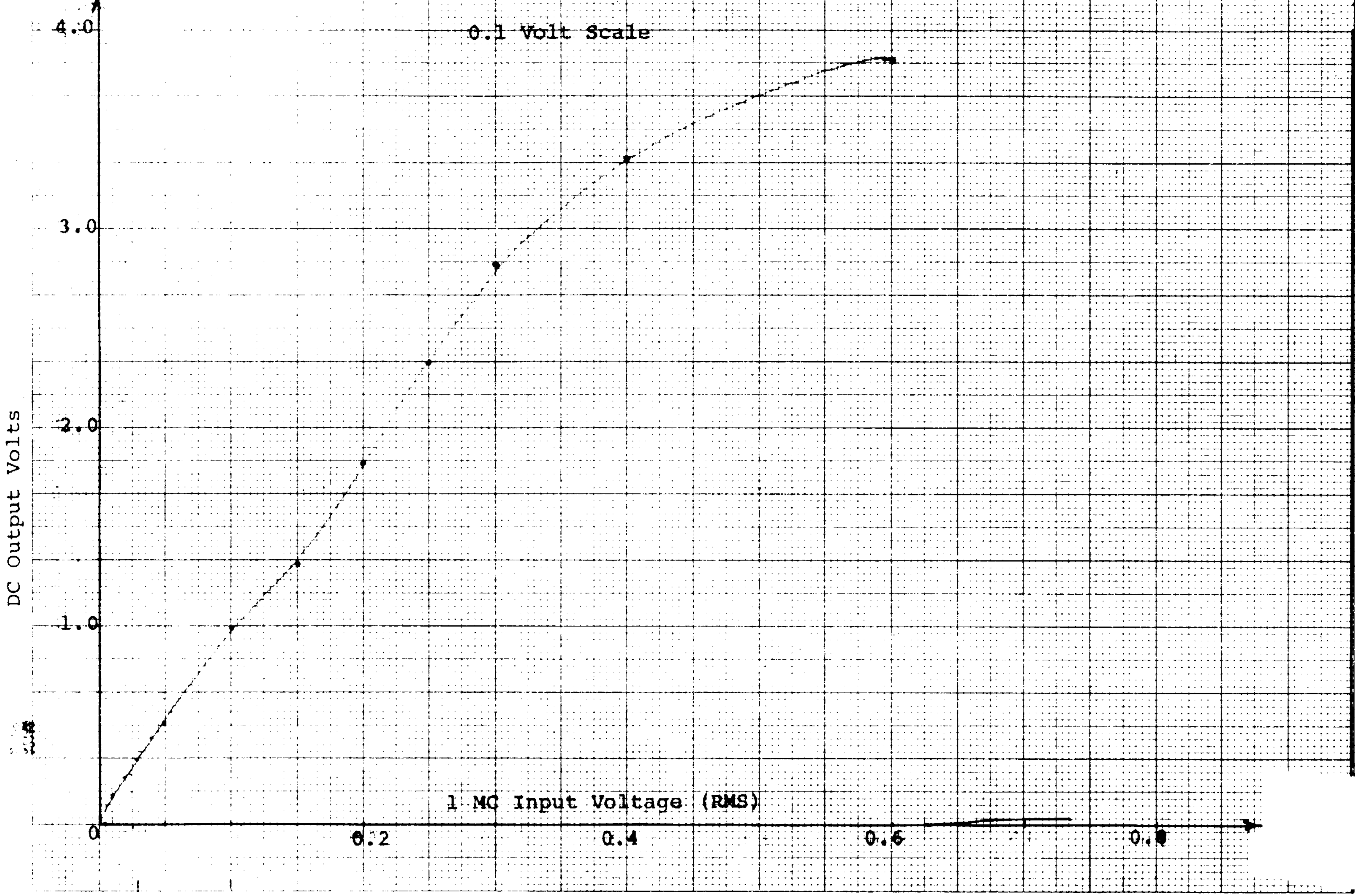

EXPERIMENT ______ TARGET ______ NAME ______ DATE ______

Transmit							
Channel	Room 138 T-	Jct. Tank Top T-	Power Amp. IN T-	Power Amp. Out TT-	Distribution Unit IN R-	Distribution Unit OUT R-	Room 138Y R-
1							
2							
3							
4							

	Receive 138Y HP. Voltmeter IN	Receive 138Y HP. Voltmeter DC OUT Scale	V_x V_y volts 0	X Y Z	DC Ampl.	Paper Tape Sens.-Speed	Mag. Tape Calb (FM) f-	f_o	f+	±level
1										
2										
3										
4										
5										

FIG. 3-4. CHECKOUT (V = SINE WAVE) SHEET

Take FM Reproduce and FM Filter from odd channels.

Replace them with Direct Reproduce and Short Cards.

Run the tape in high speed and record mode.

Apply 0 volt to the input of the channel under test.

Monitor the output with a counter and read 108 kc/s ($\pm$ 1%).

In case of having a different frequency from 108, adjust with a Isolated Screw Driver varying the upper part of that channel in the first two rows of controls (accessible in the front part), namely input rows, adj-Δ.

Apply $\pm$ 2 volts.

Monitor and read 108 kc/s $\pm$ 40%.

for + 2 V.	read	151 kc/s ($\pm$ 1%)
for - 2 V.	read	65 kc/s ($\pm$ 1%)

In case of any adjustment needed, vary the part of the corresponding channel located in the second row of the input rows, namely LEVEL.

NOTE: Front Controls

0	0	0	0	0	0	... 0	Adj- Δ	← Center freq.
0	0	0	0	0	0	... 0	LEVEL	← Sensitivity
1	2	3	4	5	6	14		

INPUT

0	0	0	0	0	0	... 0	LEVEL
0	0	0	0	0	0	... 0	Adj- Δ
1	2	3	4	5	6	14	

OUTPUT

Procedure for Experimental Work

Calibration:

1. Mount a flat-plate target
   - (a) Tighten six mounting bolts on target frame
   - (b) Tighten three bolts-nuts on transducer tower
   - (c) Stabilize transducer tower with no one moving on tank structure
2. Run at constant
   - (a) Elevation Y_o
   - (b) Horizontal Setting X_o

   Record mixer output (phase) for 0^o angle of incidence at one mc. After recording signal levels and shape on standard sheet (enclosed).
3. Recheck and adjust if necessary. Horizontal parallel positions of target and transducer carriage. Rerun until exact.
4. Record received signal levels at 10, 20, 30, 40 K ft. equivalent elevations and check for lowest signal levels.

Actual Run:

1. (a) Replace flat plate with target and ready experiment as in Calibration - 1
   (b) Recheck horizontal velocity with calibration chart.
2. Record voltage level and wave shapes on standard sheet.
3. Set recorder levels and note all constants.
4. Run experiment and check intermittently the signal level and shapes.

Note: Standard Magnetic Tape Recorder calibration procedure is given on the following sheet.

Operating Instructions

1. Tighten all bolts and nuts; grease X, Y rails; lubricate all gears.

2. Place both targets* (4' x 6') (secure all 8 bolts in bolt positions marked yellow/red) with calibration plate hung in front of transducers and two bolts at desired distance from flat face of transducer with altimeter (center) beam looking vertically or at desired angle at plate.

3. Make sure the following encoders are working:

   (a) Pitch angle
   (b) X-position
   (c) Y-position

4. Wait for Calibration signal Recording.

After Finishing Experiment Data

1. Pull out transducer package from water after

   (a) Removing pitch angle encoder rod
   (b) Secure your protector angle readings

2. Pull out target above water after removing bolts at both top ends.

Electrical On Top of Tank

1. Turn on the Power Supply Switch

2. Secure all three encoder operations

3. Secure all three nixie tube inputs from respective encoder outputs.

*Both positioning bolts in tower top must be in place.

CHAPTER IV

ULTRASONIC SIMULATION VIS-A-VIS FULL SCALE RADAR RETURN

For the last ten to fifteen years it has been well established (Hayre and Vroulis, 1968) that ultrasonic simulation of linearly polarized radar return from all sorts of surfaces, objects and volumes is not only valid but a very practical and inexpensive analog tool. Furthermore, recent studies (Hayre, et al, 1969, Hayre, 1968, Hayre and Avgeris, 1968) have further shown that it is also possible to obtain absolute values of the radar cross-section of targets using this simulation in addition to being able to calculate the return for circularly polarized field from the simulation of linear polarization radar return.

A very brief summary of basic theory is given here as a refresher to those readers not familiar with this technique. For scalar waves the classical equations and boundary conditions are:

EM Waves

$$\nabla^2 \binom{E}{H} = \mu \epsilon \frac{\partial^2 \binom{E}{H}}{\partial t^2}$$

$$\bar{n} \times (\bar{E}_1 - E_2) = 0$$

$$\bar{n} \times (\bar{H}_1 - H_2) = \bar{J}_s$$

Ultrasonic

$$\nabla^2 \binom{P}{U} = \rho_\ell k_\ell \frac{\partial^2 \binom{P}{u}}{\partial t^2}$$

$$P_1 = P_2$$

$$\bar{n} \cdot (\bar{u}_1 - u_2) = 0$$

where

$\binom{E}{H} = \binom{\text{Electric}}{\text{Magnetic}}$ field vectors

$\bar{n}$ = outward surface normal

ϵ = dielectric constant

μ = permeability

$\binom{P}{U} = \binom{\text{Pressure field scatter}}{\text{Particle Velocity}}$ Vector

ρ_ℓ = density

k_ℓ = compressibility of medium

Thus these are identical for the same time variation and the same form of the wave front, i.e., cylindrical, spherical or plane waves, etc., so long as the boundary conditions are not too dissimilar. This criterion is satisfied in this experiment as discussed later in this chapter.

Furthermore, the scattered scalar fields E and p are both given by the Helmholtz theorem in an identical form as:

$$\binom{E}{p}(R) = \frac{1}{4\pi}\oint\left(\binom{E}{p}_s \frac{\partial\psi}{\partial n} - \psi\frac{\partial\binom{E}{p}}{\partial n_s}\Big|_s\right)ds$$

where $\psi = e^{j(kR'-\omega t)}/R'$ (Green's Function in general)

S = Surface illuminated

$|_s$ = Evaluated at the Surface S

Continuing in this fashion, one can also write the reflection coefficient R for oblique incident plane wave for EM waves versus ultrasonics, as follows:

$$R = \frac{Z_2 \sec\theta_2 - Z_1 \sec\theta_1}{Z_2 \sec\theta_2 + Z_1 \sec\theta_1}$$

where Z_2 = Impedance of Medium 2 $= \sqrt{\frac{\mu_2}{\epsilon_2}} = \rho_2 C_2$

Z_1 = Impedance of Medium 1 (incidence wave) $= \sqrt{\frac{\mu_1}{\epsilon_1}} = \rho_1 C_1$

C_i = Velocity of Sound in Medium i

Of course **it** is obvious that this is the case for the perpendicularly polarized em wave, but it can be readily seen that in order to apply this unique case to horizontally polarized case, one needs to modify the Z_i as

$$Z_i' = Z_i \cos^2\theta_i$$

This argument may further be extended to losses in the second medium, namely the model material in case of ultrasonics and the lunar or earthly surface material in the case of radar, in order to account for exact losses or penetration for some other applications.

It is very pertinent to comment on the radar return statistics and its simulated counterpart in ultrasonic data that all such parameters as:

a) Range of fading

b) Rate of fading

c) Doppler statistics

d) Statistical mean and σ , and

e) Spatial and temporal fading

have been successfully simulated for various applications varying from signature, classification of earth resources to guidance and control signals, etc.

Finally, it has been shown that plane wave scattering from statistically two or three dimensional rough surfaces for radar and ultrasonic, is identical phenomena (Tolstoy and Clay, 1966 [ultrasonic], Beckmann and Spizzichino, 1963[radar]). For further details, the reader is referred to these textbooks. Now one raises the question as to how do both of these cases compare from the standpoint of signal statistics in terms of various parameters such as beam shapes, range, surface features, etc. This is discussed in the following paragraphs.

The modeling of targets for low altitude radar reflectivity study must meet the following requirements in order for such a model to appropriately represent the real target in ultrasonic simulation:

a) Beam shape and target area illuminated

b) Signal wave shape and wave front

c) Specular reflection

d) Shadowing versus angle of incidence

e) Diffraction

f) Range effects

g) Target surface significant features

h) Repeatability of experiment

In both cases of the radar reflectivity simulation, one for the lunar landing site and the other for the Hummocks area, these criterion were met by these procedures:

a) The beam shapes of the transmitting and receiving transducers were shaped to be as close as possible to those for the corresponding LM radars.

b) The x-, y-, z-scale factors were so selected as to illuminate an area on the model surface identical to that illuminated on the actual surface by radar.

c) The surface heights were so modeled that the flat specular areas were reproduced identically, and the general major surface features were also modeled to scale. Then the general roughness was added by using mesh 200 sand, whose particles are 0.0...mm or less in size, thus allowing diffracting points to be more or less identically modeled.

d) The major shadowing areas were appropriately considered in general modeling such that the percent model surface in shadow for a given angle of incidence was approximately the same as would be the case for full scale radar experiment.

e) Range effects are well established for the transducer case and in fact, in this simulation both the radar and the transducers were operating in the intermediate field at the lowest altitude, and in far field at higher altitudes.

At times various NASA Manned Spacecraft Center personnel and their contractors were eager to see how our experimental setup was able to reproduce radar associated results. Thus many types of short demonstrations were given for them and one of these is discussed below. In case of CW transmitter, if one moves the transmit-receive transducer package away from a flat aluminum reference plate, one obtains a continuously decaying return. This is demonstrated in Fig. 4-1. Similarly, at various times the repeatibility of the experiment was demonstrated. A typical graph of the received signal level versus time by moving the transducer package along the target at a fixed altitude was recorded on Fig. 4-2, which shows the results of forward motion.

Thus a complete theoretical justification was verified for simple classical flat plate and extremely meaningful radar return and their target surfaces.

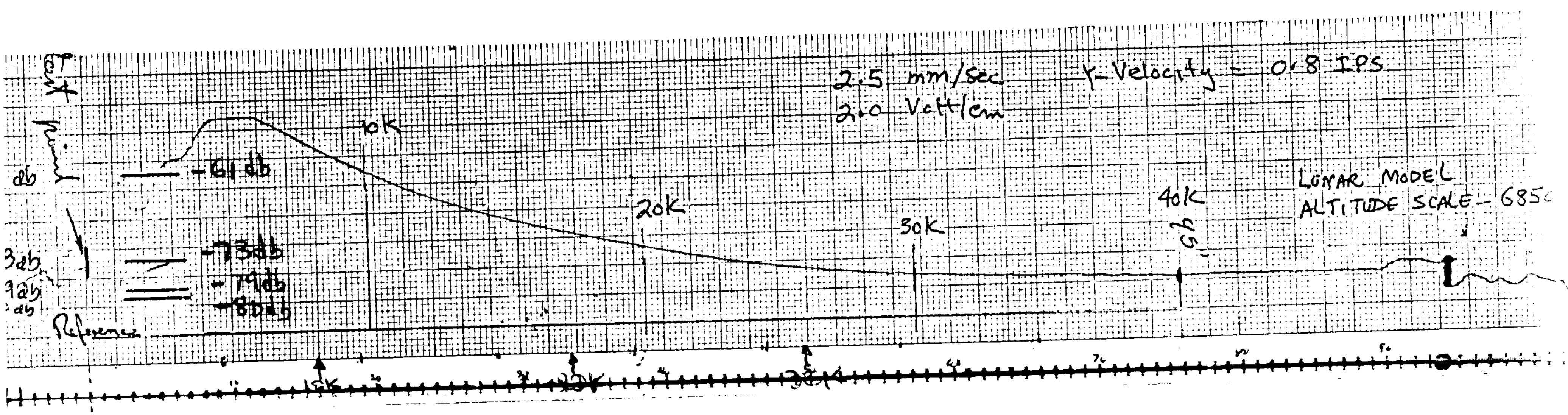

Fig. 4-1. Simulated Radar Return Vs. Altitude at 1 MC-CW

Transmit-Receive Package Moving Along at +X Direction

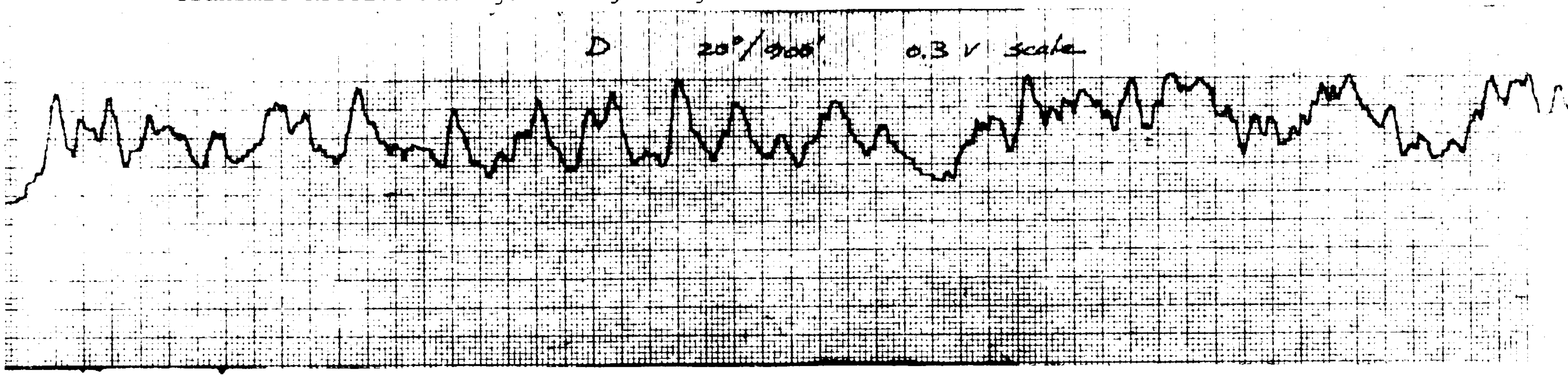

Transmit-Receive Package Moving Along at -X Direction

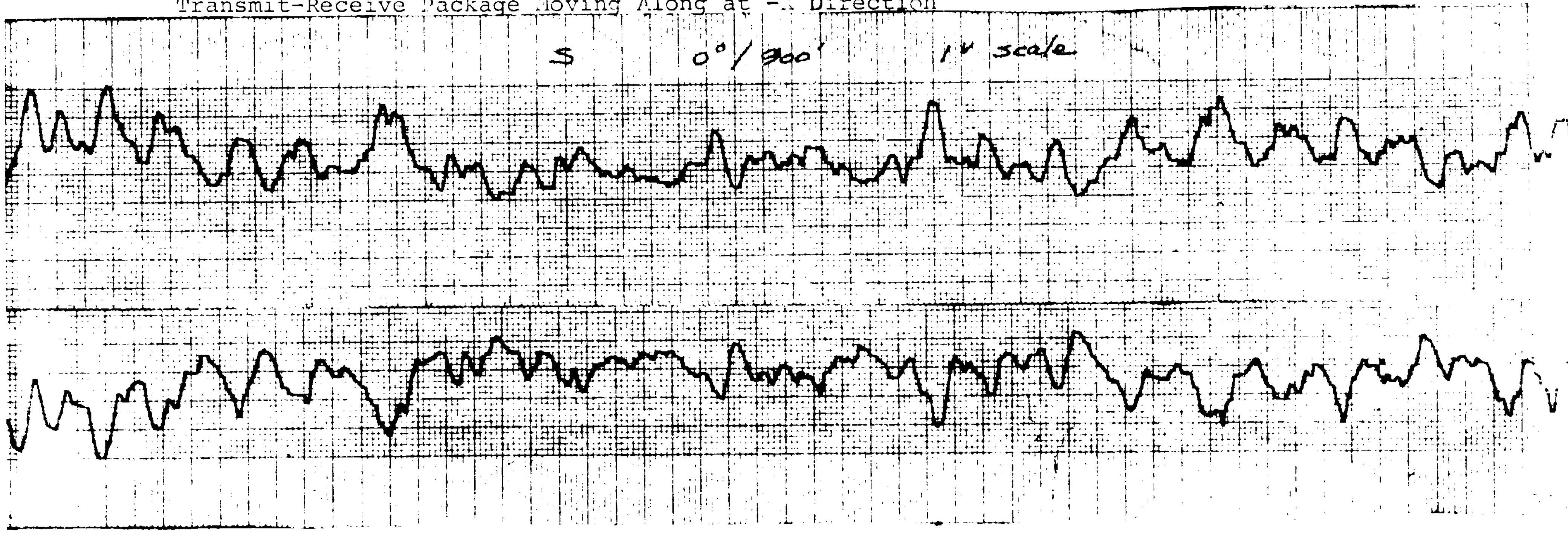

Fig. 4-2. Exact Reproduction of CW Received Signal Level in Either Direction of the Motion of the Transmit-Receive Package Along Target Surface At A Fixed Altitude

CHAPTER V

DATA ANALYSIS AND CONCLUSIONS

The amplitude of the continuous wave 1.0 megacycle/sec signal backscattered by both the Hummocks area (WSMR) and lunar landing site P-II-6 and 8 models was detected by the HP EL 400 voltmeter in the form of a direct current voltage varying with the input amplitude. The dc voltage of one volt corresponds to the full scale reading of each scale of the voltmeter, and its linearity for values of input above the full scale values is discussed in Chapter III. This signal was both paper tape recorded on Sanborn 150 and magnetic tape recorded (FM) on Precision Model PI 214. The analysis discussed in this chapter deals with exclusively the paper tape recorded signals as shown in the Appendix because the magnetic tape recorded signals were transmitted to NASA Manned Spacecraft Center.

The paper tape recorded signal is recorded on a millimeter scale paper at 5 mm/sec in most of the cases unless otherwise noted in data tables. Each curve was read at every millimeter division and its mean and standard deviation was calculated using Wang computers. In each case the values were then referred to one volt scale reading of the 400 EL voltmeter-detector for the sake of uniformity and then converted to actual voltage scale as shown in Tables A-1 and A-2. Furthermore, these voltage levels for the mean and standard deviation were then used to compute mean minus standard deviation, mean, and mean plus standard deviation value so that these may then be refered to a flat plate reference. In case of the lunar model, each reflectivity curve (cross-section versus angle of incidence) was refered to 10 K feet flat plate reference and is presented in Fig. A-3. At the same time each altitude data may also be refered to as flat plate reference at that altitude and in order to enable one to obtain this information, special scales are added on the right hand side of Fig. A-3 showing the corresponding new referenced scales such as (refer to Fig. A-3):

10 K Reference Plate -- Scale of Fig. A-3

20 K Reference Plate -- Scale of Fig. A-3 plus +7.9 db

30 K Reference Plate -- Scale of Fig. A-3 plus +14.9 db

40 K Reference Plate -- Scale of Fig. A-3 plus +19 db

Thus it is relatively easy to refer these values in Fig. A-3 to any one of these or any other reference, for that matter.

The final radar reflectivity simulation data for the lunar surface landing site P-II-6 and 8 model for altitudes 10, 20, 30 and 40 K ft is presented in two figures, Fig. A-2 and Fig. A-3. Figure A-3 shows the actual data with plus and minus sigma values around the mean in db, whereas Fig. A-2 shows a smoothed curve fit to Fig. A-3 actual data with projected plus and minus sigma values for each smoothed mean point so obtained. It is pertinent to add that on a decible scale the mean plus sigma and mean minus sigma are not symmetrically located around the mean as would be the case in a linear voltage or power reflectivity data plot, because of the logarithmic operation not being a linear operation.

All the steps of this calculation are shown in Table A-1, whereas the actual radar simulated reflectivity data for the lunar landing site are given in Figs. A-4 through A-13.

The paper tape recorded data for Hummocks area (WSMR) was also recorded on a millimeter grid paper at 5 mm/sec most of the time and the sampling, reading, as well as the analysis of the data was identical to that for the lunar landing sites. The actual process of raw data, its processing is shown in Table A-2, and the end result of simulated radar reflectivity (radar cross-section normalized to 1,000 ft. flat plate data) versus the altitude for 0° and 20° angles of incidence are presented in Fig. A-20. The values at 100, 200 and 300 feet altitudes had to be corrected for parallax errors introduced by the positioning of transmit-receive transducers. For instance, these transducers-package were originally designed for use at 400 to 25,000 ft. altitudes, and thus their pointing error is expected to be introduced at distances corresponding to approximately 10" from the target face or approximately (10/12) x 500 = 417 ft. simulated altitude or below. This parallax correction for altitudes below 400 ft. is shown in Fig. A-21, and the extrapolation curves forming the basis of this work are shown in Fig. A-19.

The final simulated reflectivity data for the Hummocks area (WSMR) is presented in the form of the mean radar cross-section versus altitude with mean plus sigma and mean minus sigma points shown on the same graph for each zero and 20 degree angle of incidence. No smoothing was done but an average smooth curve was drawn to show the variation of the mean values.

Conclusions

The simulated lunar reflectivity data versus angle of incidence from zero to fifty degrees shown in Fig. A-3 and Fig. A-2 show that such a mean smooth curve for radar cross-section versus angle is a very gross measure of the surface effect. In fact, the mean value may vary as much as ± 1.4 db from the smooth fitted curve. A more significant fact of this investigation is that the ± sigma points are at the farthest ± 4 db above and below the smoothed curve, noting that the large plus-minus excursions do not occur at the same angle of incidence. For instance, the 10 K curve has +3.2 db plus one sigma excursion above the smooth curve at $\varphi = 45^{\circ}$, -2.8 db at $\varphi = 30^{\circ}$, +3.6 db at $\varphi = 25^{\circ}$, +2.8 db at $\varphi = 20$, +2.4 at $\varphi = 15^{\circ}$, -2.75 db at $\varphi = 10^{\circ}$, -3.6 db at $\varphi = 5^{\circ}$, and -4.1 db at $\varphi = 0^{\circ}$. Similarly, the 20K, 30K and 40K curves show realistic excursions of the mean and mean plus and mean minus signal values.

The mean for 20K curve vary almost consistently from the smoothed curve fit at angles from 20° to 40° whereas those at 30K and 40K almost fall on the smooth fit. The reasons for this are quite understandable in view of the fact that at higher altitudes, the radar illuminates larger areas and the receiver averages the return from a large area with a possible wide variety of surface features. Hence the higher altitude data is much more smoothed than that taken at low altitude data. Furthermore, the sigma (standard deviation) values show an increas as the angle approached zero as well as the altitude is decreased. This is also as expected because the area seen by the radar at low altitudes is smaller than that at high altitudes, and it is equivalent to a small sample and, hence, the variability from the mean is expected to be large. It must be noted that there is a weak consistent increase in plus-minus sigma values with a decrease in altitude for the lunar surface model as opposed to a relatively smooth surface because the salient features of the surface dominate the return.

These results show an excellent correlation between the variations of the mean return and sigma values with altitude and angle of incidence. Another major result is that the same surface seems smoother at zero degree angle of incidence at lower altitudes of 10 and 20 K ft. as opposed to 30 and 40 K because of the flatness of small area seen by the low altitude positioned radar. In summary, all the curves simulated extremely well the expected radar results for the lunar landing sites P-II-6 and 8 at the 10 to 40 K ft. altitudes, and offer a very effective means for checkout of LM gear as opposed to assumed reflectivity curves. These are also consistent with theoretical studies made earlier.

The simulated radar reflectivity data versus altitude varying from 100 ft. to 1,000 ft., and refered to 1,000 ft. flat plate data appear in Fig. A-20. The detailed calculation results are listed in Table A-2. The mean for this experiment is interestingly very close to the smooth curved fitted to the data and this was expected as the Hummocks area (WSMR) is relatively flat except for the flat top sand piles. For radar purposes, such a site may well be assumed to be flat. The maximum excursion of mean from the smooth curve is no more than ± 1 db, whereas the increase in standard deviation with decrease in altitude is consistent with the relatively flat area theory and experimental work by many authors (Hayre, 1962; Hayre and Tong, 1963). It is noteworthy that the plus/minus sigma spread is of the order of -3 to -7 db as the altitude goes down from 1,000 ft. to 200 ft. for zero degree angle of incidence as opposed to -2.8 db to -6 db for 20 degree angle of incidence for the same corresponding altitude variations. This is also as expected because even for such a smooth looking surface the sides of the flat top send facts to reduce the radar return significantly, as fewer flat facets look toward the radar. In summary, these results seem to support the theory and previous experiment and in fact show a very definite reliable variation with altitude and angle of incidence. NASA Manned Spacecraft Center and White Sands Missile Range radar reduced data was not available at the time of the preparation of this report, but a comparison of some preliminary results with these simulated results was indeed excellent.

In conclusion, the ultrasonic simulation is a very reliable, laboratory controlled, inexpensive and quick method of evaluating a radar system and for checking an already designed system for various surface effects.

REFERENCES

Beckmann, P. and A. Spizzichino. The Scattering of Electromagnetic Waves from Rough Surfaces. New York: McMillan Co., 1963.

Hayre, H. S. and T. G. Avgeris. Acoustic Simulation of Apollo Radar Cross-Section Using 1/48 Plastic Model. University of Houston, Dept. of Electrical Engineering, Tech. Rept. TR-68-15, August, 1968.

Hayre, H. S. Lunar Terrain and Reflectivity Study. University of Houston, Dept. of Electrical Engineering, Tech. Rept. TR-68-17, October, 1968.

Hayre, H. S. and G. Vroulis. Analogies Between EM and Acoustic Waves. University of Houston, Dept. of Electrical Engineering, Tech. Rept. TR-68-19, November, 1968.

Hayre, H. S. and S. Y. Shen. Ultrasonic Simulation of Apollo Radar Cross-Section. University of Houston, Dept. of Electrical Engineering., Tech. Rept. TR-69-2, January, 1969.

Hayre, H. S. and A. Tong. Radar Reflectivity Model for LEM. University of Houston, Dept. of Electrical Engineering, Tech. Rept. TR-67-7, March, 1967.

Hayre, H. S. and A. Tong. Surface Models. University of Houston, Dept. of Electrical Engineering, Tech. Rept. TR-67-15, August, 1967.

Tolstoy, I. and C. S. Clay. Ocean Acoustics. New York: McGraw-Hill, 1965.

APPENDIX A

FIGURES AND TABLES

FIGURES - APPENDIX A

LIST OF TABLES

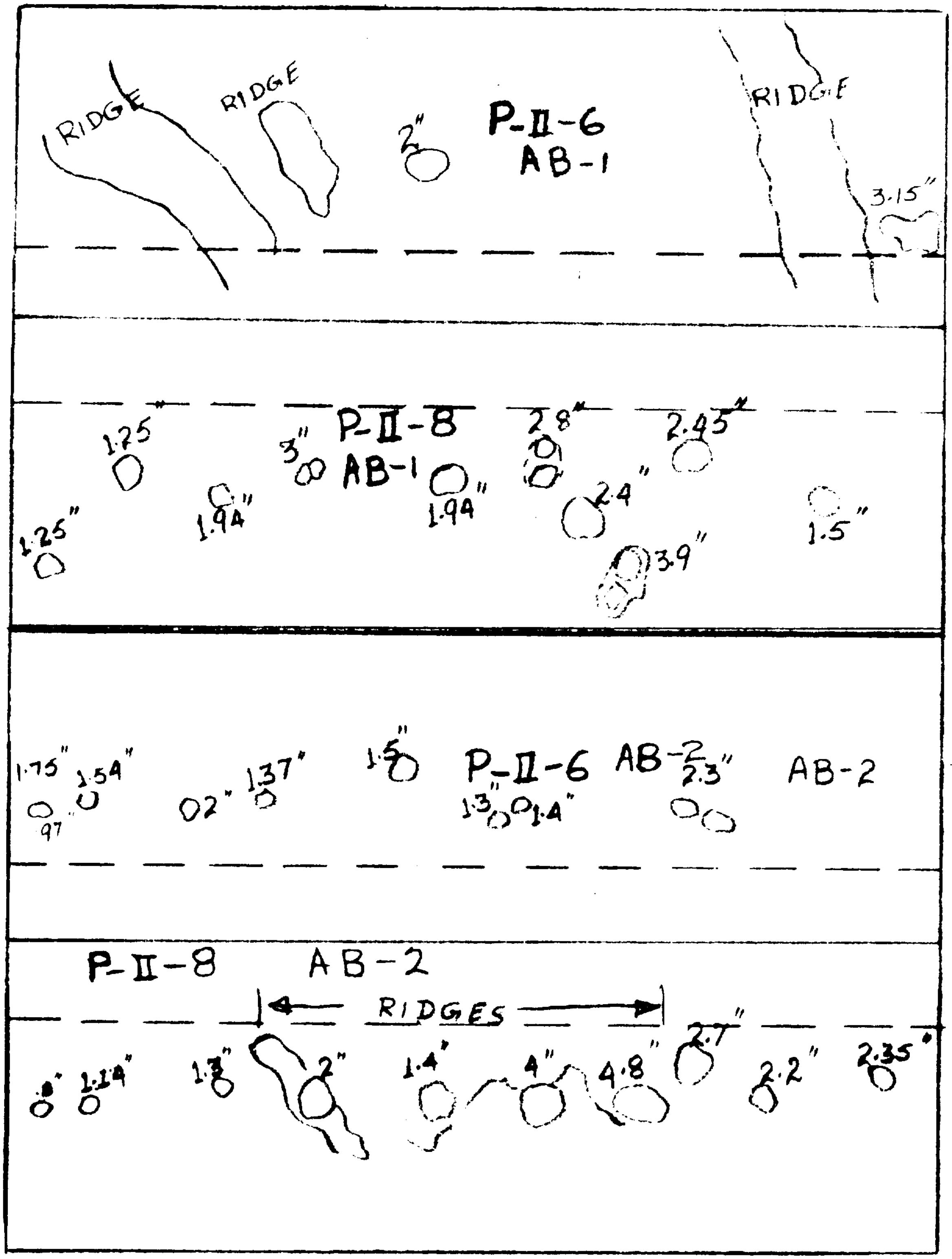

FIG. A-1 LUNAR LANDING SITE SURFACE MODEL P-II-6 & 8, A,B
Scale 6850:1

FIG. A-2. SIMULATED DATA VERSUS INCIDENCE ANGLE FOR LUNAR SURFACE P-II-6 & 8 MODEL (Smooth)

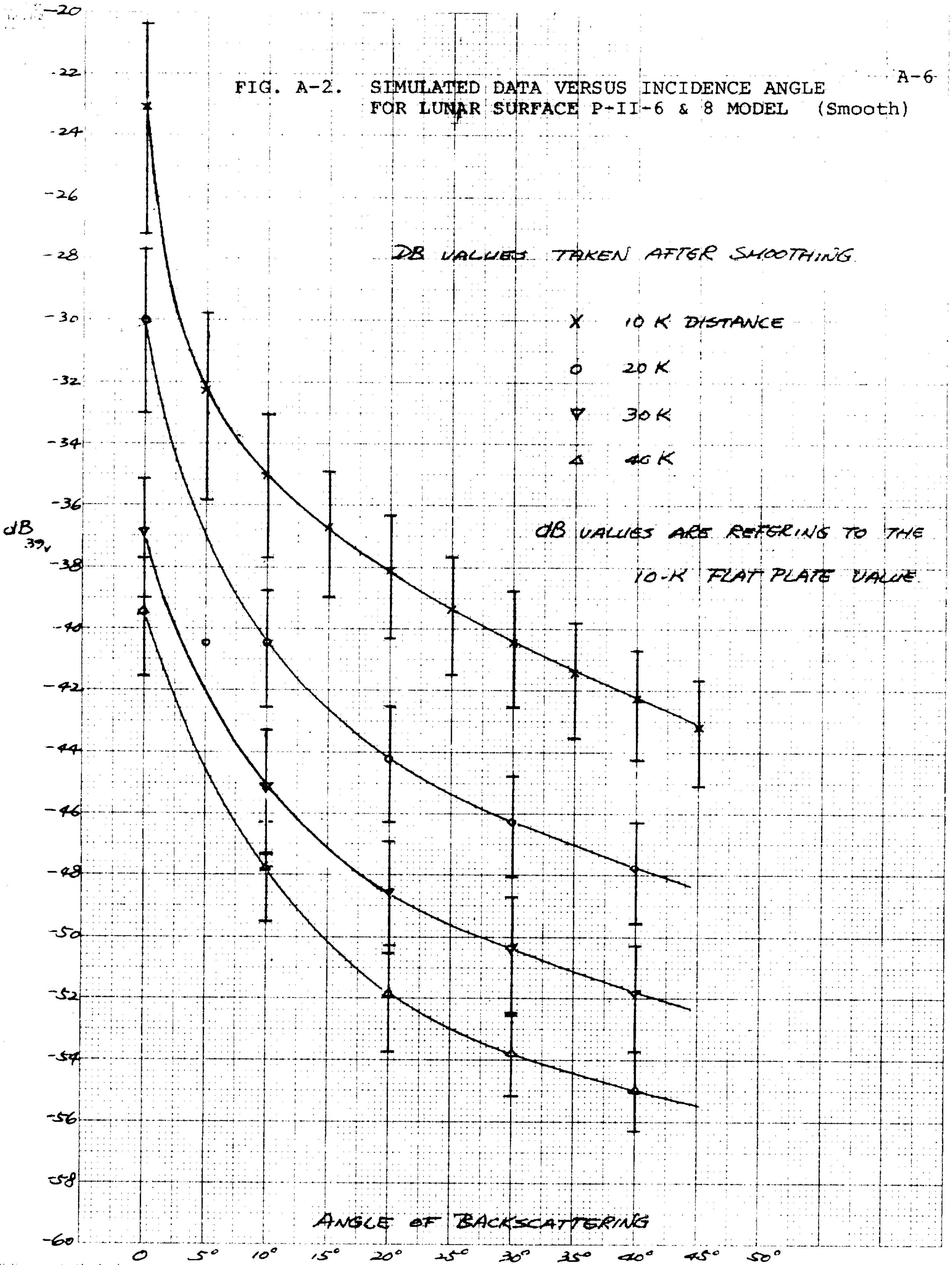

20 Squares to the Inch

FIG. A-3. SIMULATED DATA VERSUS INCIDENCE ANGLE FOR LUNAR SURFACE P-II-6 & 8 MODEL (Actual)

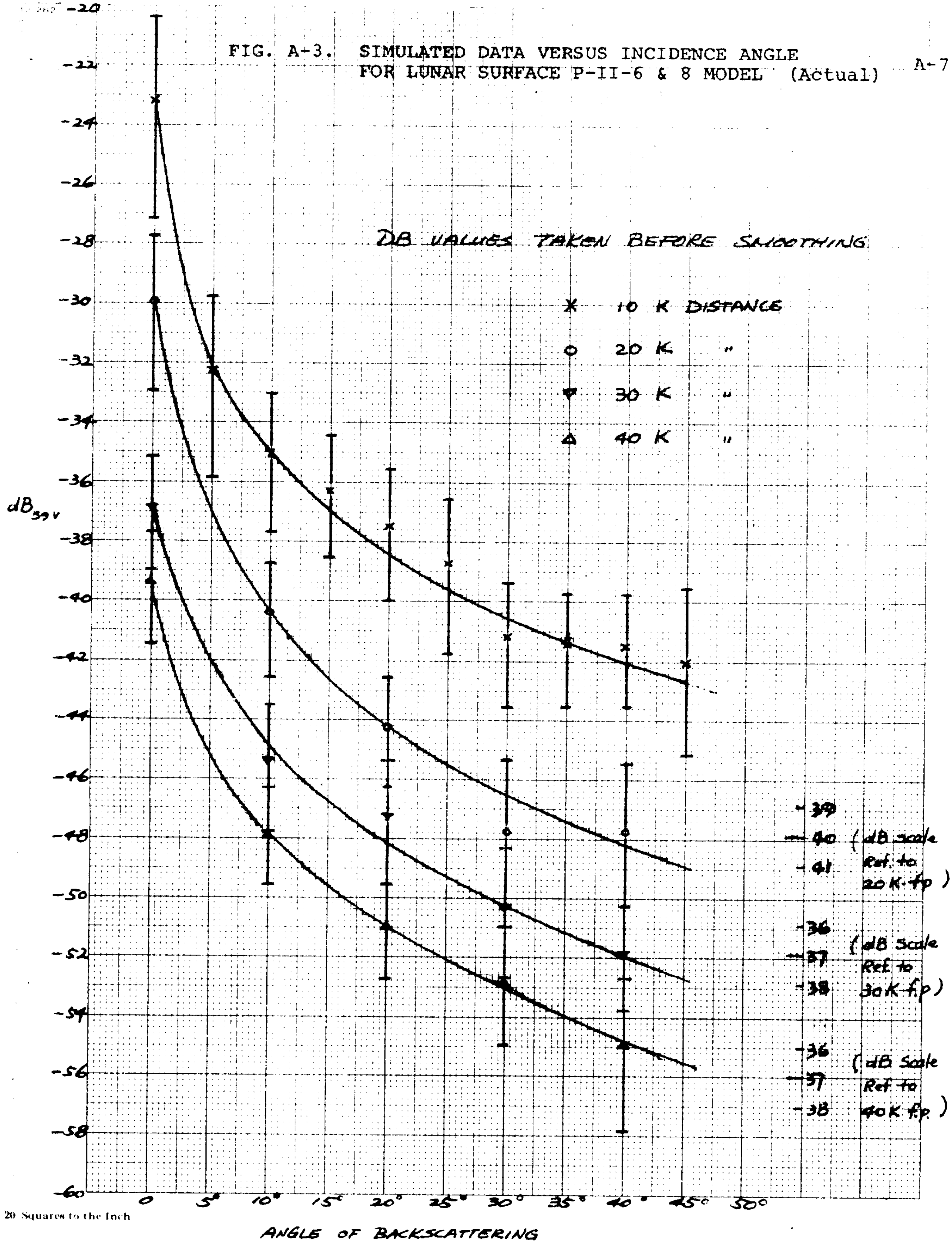

20 Squares to the Inch

TABLE A-1

SUMMARY OF SIMULATED REFLECTIVITY DATA FOR LUNAR SURFACE P-II-6 & 8 MODEL

Dist. (feet)	Run	Angle (degrees)	Actual voltage (volts) Mean m	Std. Dev σ	$m + \sigma$	$m - \sigma$	dB above 39 volts (Ref. 10K F.p. voltage) $m + \sigma$	m	$m - \sigma$
10K	4	0	2.72	1.01	3.73	1.71	-20.39	-23.13	-27.16
	5	5	0.95	0.32	1.27	0.63	-29.75	-32.27	-35.84
	6	10	0.69	0.18	0.87	0.51	-33.03	-35.04	-37.68
	10	15	0.57 (0.60)	0.13 (0.14)	0.7	0.44	-34.92	-36.72 (-36.26)	-38.96
	11	20	0.485 (0.52)	0.11 (0.13)	0.595	0.375	-36.32	-38.12 (-37.51)	-40.34
	15	25	0.42 (0.45)	0.092 (0.13)	0.512	0.328	-37.64	-39.36 (-38.76)	-41.50
	16	30	0.37 (0.34)	0.08	0.45	0.29	-38.76	-40.45 (-41.19)	-42.57
	20	35	0.33	0.07	0.40	0.26	-39.80	-41.44	-43.52
	21	40	0.3 (0.33)	0.06 (0.07)	0.36	0.24	-40.69	-42.28 (-41.44)	-44.22
	25	45	0.27 (0.31)	0.052 (0.10)	0.322	0.218	-41.66	-43.20 (-42.00)	-45.06

(Numbers in parentheses are values direct from calculation)

(Sheet 1 of 5)

TABLE A-1 (CONT'D)

SUMMARY OF SIMULATED REFLECTIVITY DATA FOR LUNAR SURFACE P-II-6 & 8 MODEL

Dist. (feet)	Run	Angle (degrees)	Actual voltage (volts) Mean m	Std.Dev σ	m + σ	m - σ	dB above .39 volts (Ref. 10K f.p. voltage) m + σ	m	m - σ
20K	3	0	1.24	0.36	1.60	0.88	-27.74	-29.96	-32.94
	7	10	0.37	0.08	0.45	0.29	-38.76	-40.47	-42.57
	12	20	0.24	0.05	0.29	0.19	-42.57	-44.21	-46.24
	17	30	0.19 (0.16)	0.035 (0.05)	0.225	0.155	-44.77	-46.24 (-47.74)	-48.02
	22	40	0.16	0.03 (0.04)	0.19	0.13	-46.24	-47.74	-49.55
	27	50	0.13 (0.05)	0.022 (0.01)	0.152	0.108	-48.19	-49.55 (-57.85)	-51.16
30K	2	0	0.56	0.12	0.68	0.44	-35.18	-36.87	-38.96
	8	10	0.217 (0.21)	0.05	0.267	0.167	-43.28	-45.10 (-45.37)	-47.36
	13	20	0.146 (0.17)	0.03 (0.04)	0.176	0.116	-46.91	-48.54 (-47.21)	-50.53
	18	30	0.118 (0.12)	0.025 (0.03)	0.143	0.093	-48.72	-50.38 (-50.24)	-52.44
	23	40	0.10	0.02	0.12	0.08	-50.24	-51.83	-53.76
	28	50	0.09 (0.03)	0.015 (0.01)	0.105	0.075	-51.40	-52.73 (-62.28)	-54.32

(Numbers in parentheses are values direct from calcul

TABLE A-1 (CONT'D)

SUMMARY OF SIMULATED REFLECTIVITY DATA FOR LUNAR SURFACE P-II-6 & 8 MODEL

Dist. (feet)	Run	Angle (degrees)	Actual voltage (volts) Mean m	Std. Dev σ	$m + \sigma$	$m - \sigma$	dB above 39 volts (Ref. 10K f.p. voltage) $m + \sigma$	m	$m - \sigma$
40K	1	0	0.42	0.09	0.51	0.33	-37.68	-39.36	-41.45
	9	10	0.16	0.03	0.19	0.13	-46.24	-47.74	-49.55
	14	20	0.10 (0.11)	0.02	0.12	0.08	-50.24	-51.83 (-51.00)	-53.76
	19	30	0.08 (0.09)	0.012 (0.02)	0.092	0.068	-52.56	-53.76 (-52.74)	-55.17
	24	40	0.07	0.01 (0.02)	0.08	0.06	-53.76	-54.92	-56.26
	29	50	0.065 (0.03)	0.009 (0.01)	0.074	0.056	-54.44	-55.56 (-62.28)	-56.87

(Numbers in parentheses are direct from calculation

TABLE A-1 (CONT'D)

SUMMARY OF SIMULATED REFLECTIVITY DATA FOR LUNAR SURFACE P-II-6 & 8 MODEL

Scale = $\frac{1.0}{12}$ v/mm

Recorded Information					From Equation		True	Ref. Scale to 1 V.		Convert to voltage		No. of
Angle/ Dist.	V. M. Scale	Read. Ref.	ΣX	ΣX^2	m	σ	Mean	m	σ	m	σ	Read.
0/10K	3	30	1429.5	11586.75	5.374	3.84	10.374	32.75	12.12	2.72	1.01	265
5/10K	3	25	961.5	3848.75	3.60	1.20	3.60	11.40	3.79	0.95	0.32	266
10/10K	1	25	2130.1	18980.03	8.35	2.16	8.35	8.35	2.16	0.695	0.18	255
15/10K	1	25	2019.1	15323.69	7.21	1.65	7.21	7.21	1.65	0.6	0.137	280
20/10K	1	25	1184.8	7850.92	6.24	1.56	6.24	6.24	1.56	0.52	0.13	190
25/10K	1	25	1448.6	8400.48	5.36	1.53	5.36	5.36	1.53	0.45	0.127	270
30/10K	0.3	30	2129.7	20135.41	7.92	3.50	12.92	4.09	1.10	0.341	0.075	269
35/10K	0.3	30	2043.4	19084.4	7.42	3.61	12.47	3.94	1.14	0.328	0.073	270
40/10K	0.3	30	1975	18269.34	7.59	3.55	12.59	3.98	1.12	0.332	0.074	260
45/10K	1	25	966.9	3983.35	3.72	1.23	3.72	3.72	1.23	0.31	0.102	260
50/10K	0.1	30	1629.6	14055.7	6.52	3.71	11.52	1.15	0.37	0.092	0.031	250
0/20K	3	25	963	4895.5	4.7	1.35	4.7	14.86	4.27	1.24	0.356	205
10/20K	1	25	1118.5	5115.25	4.39	0.91	4.39	4.39	0.91	0.366	0.076	255
20/20K	0.3	30	813	4105.5	4.28	1.82	9.28	2.94	0.58	0.245	0.048	190
30/20K	0.3	25	1615.8	10886.44	6.21	1.806	6.21	1.96	0.57	0.163	0.048	260
40/20K	0.3	25	1464.8	9599.18	6.23	1.41	6.23	1.97	0.45	0.164	0.038	235
50/20K	0.1	25	1286.6	7504.34	5.64	1.04	5.64	0.56	0.10	0.047	0.008	228

(Sheet 4 of 5)

TABLE A-1 (CONT'D)

SUMMARY OF SIMULATED REFLECTIVITY DATA FOR LUNAR SURFACE P-II-6 & 8 MODEL

Scale $=\frac{1.0}{12}$ v/mm

	Recorded Information				From Equation		True	Ref. Scale to 1 V.		Convert to voltage		No. of
Angle/ Dist.	V. M. Scale	Read. Ref.	ΣX	ΣX^2	m	σ	Mean	m	σ	m	σ	Read.
0/30K	1	25	1816.1	12762.83	6.73	1.43	6.73	6.73	1.43	0.56	0.119	270
10/30K	0.3	25	2133.3	17545.23	7.9	1.81	7.9	2.495	0.572	0.207	0.048	270
20/30K	0.3	25	1707.9	11284.01	6.28	1.34	6.28	1.985	0.424	0.165	0.035	270
30/30K	0.1	30	2023.5	20748.25	8.98	3.27	13.98	1.40	0.33	0.117	0.028	223
40/30K	0.1	30	1438.5	11964.25	7.45	2.54	12.45	1.24	0.25	0.103	0.021	193
50/30K	0.03	30	1704	13204.5	6.82	2.53	11.82	0.374	0.08	0.031	0.007	250
0/40K	1	25	1241.0	6507.0	5.06	0.95	5.06	5.06	0.95	0.421	0.087	245
10/40K	0.3	25	1564.0	9507.5	5.90	1.02	5.90	1.87	0.32	0.155	0.027	265
20/40K	0.1	30	2025	18231.0	7.94	2.92	12.94	1.29	0.292	0.108	0.024	255
30/40K	0.1	30	1138	7940.5	5.81	2.62	10.81	1.08	0.262	0.090	0.022	196
40/40K	0.1	30	422.5	2038.25	3.53	2.23	8.53	0.853	0.223	0.071	0.018	126
50/40K	0.03	30	883.5	4726.25	4.44	2.01	9.44	0.30	0.064	0.025	0.005	199

(Sheet 5 of 5)

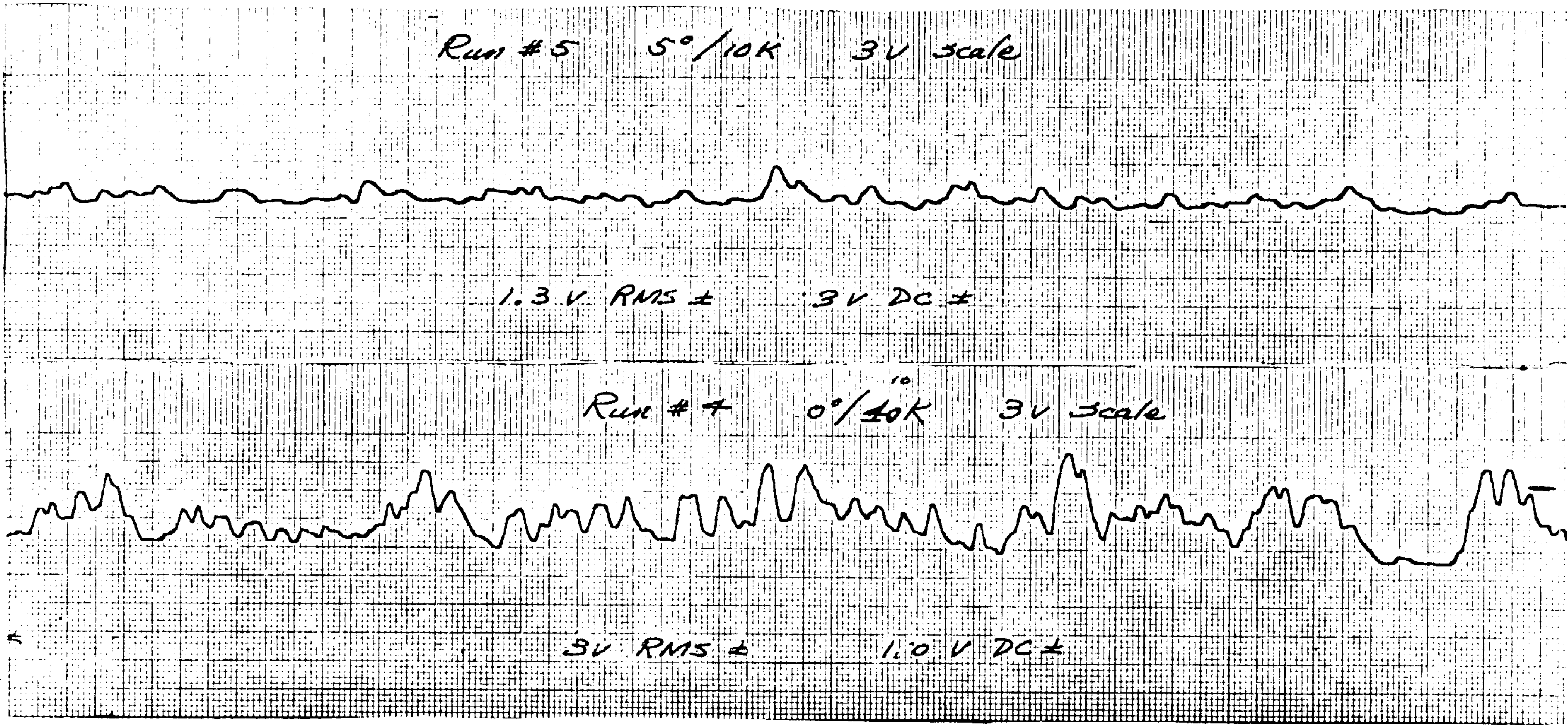

FIG. A-4 AMPLITUDE DETECTOR OUTPUT OF SIMULATED RETURN FOR LUNAR SURFACE P-II-6 & 8 MODEL
(Sheet 1 of 10)

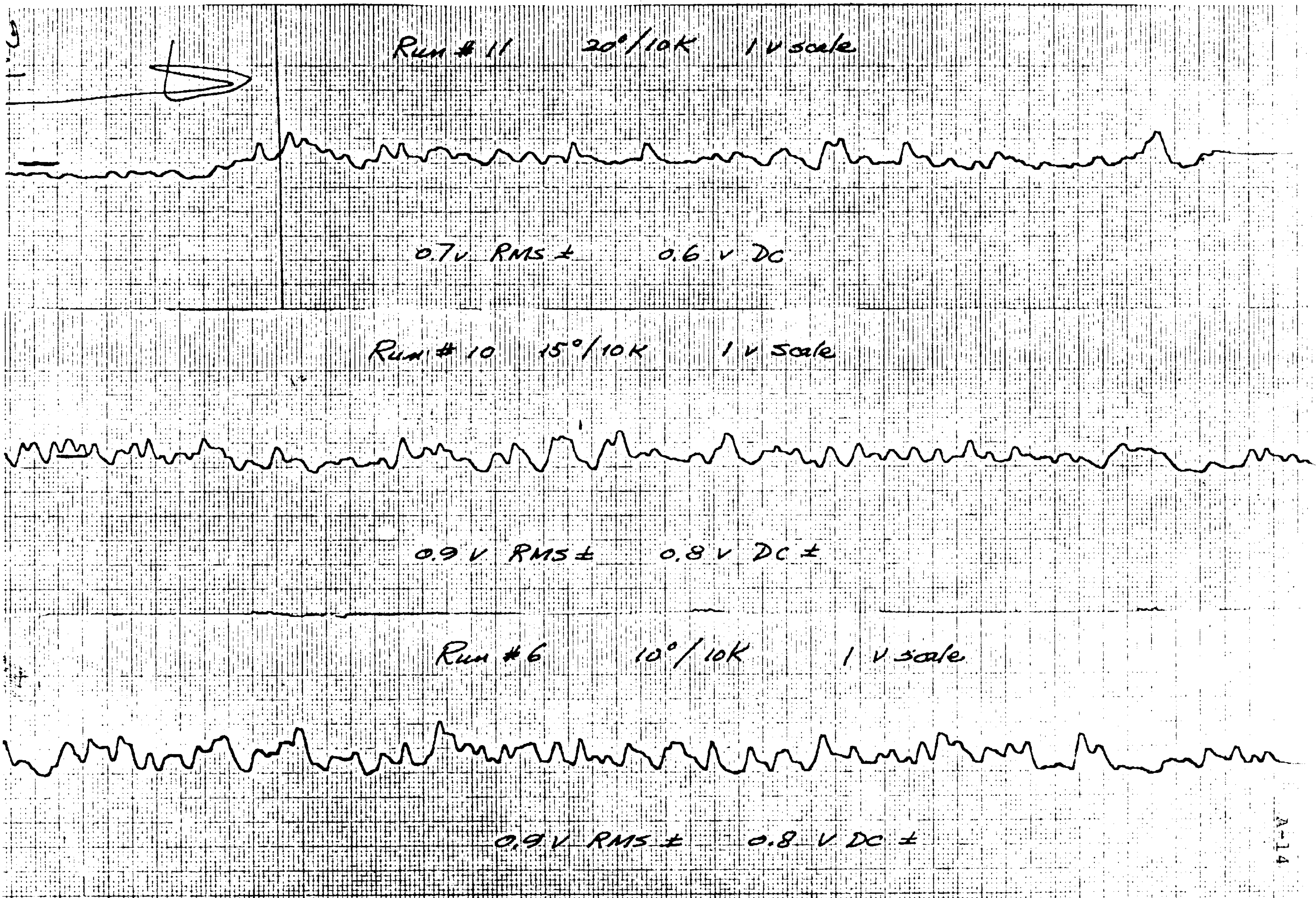

FIG. A-5 AMPLITUDE DETECTOR OUTPUT OF SIMULATED RETURN FOR LUNAR SURFACE P-II-6 & 8 MODEL (Sheet 2 of

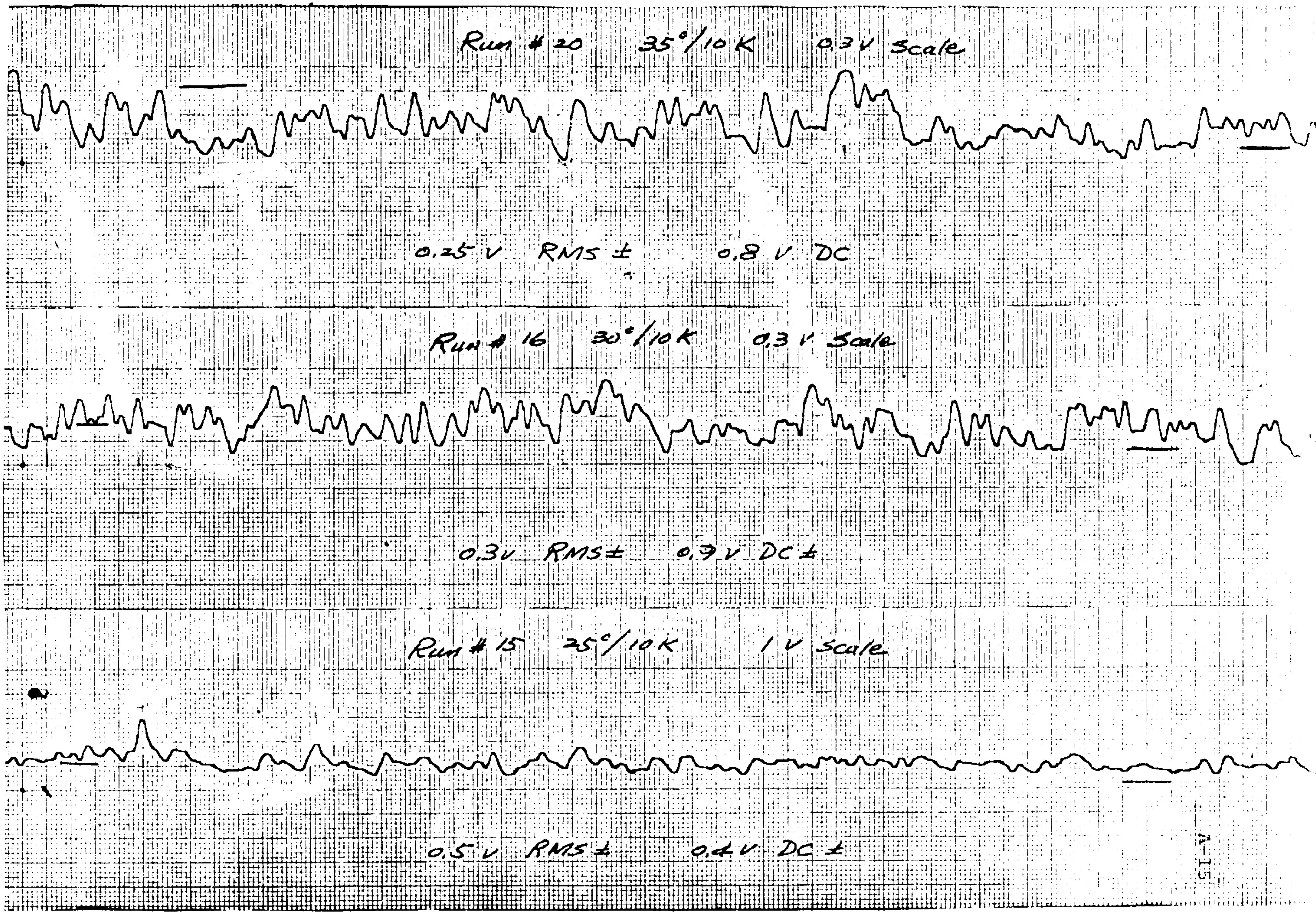

FIG. A6 AMPLITUDE DETECTOR OUTPUT OF SIMULATED RETURN FOR LUNAR SURFACE P-II 6 & 8 MODEL (Sheet 3 of 10)

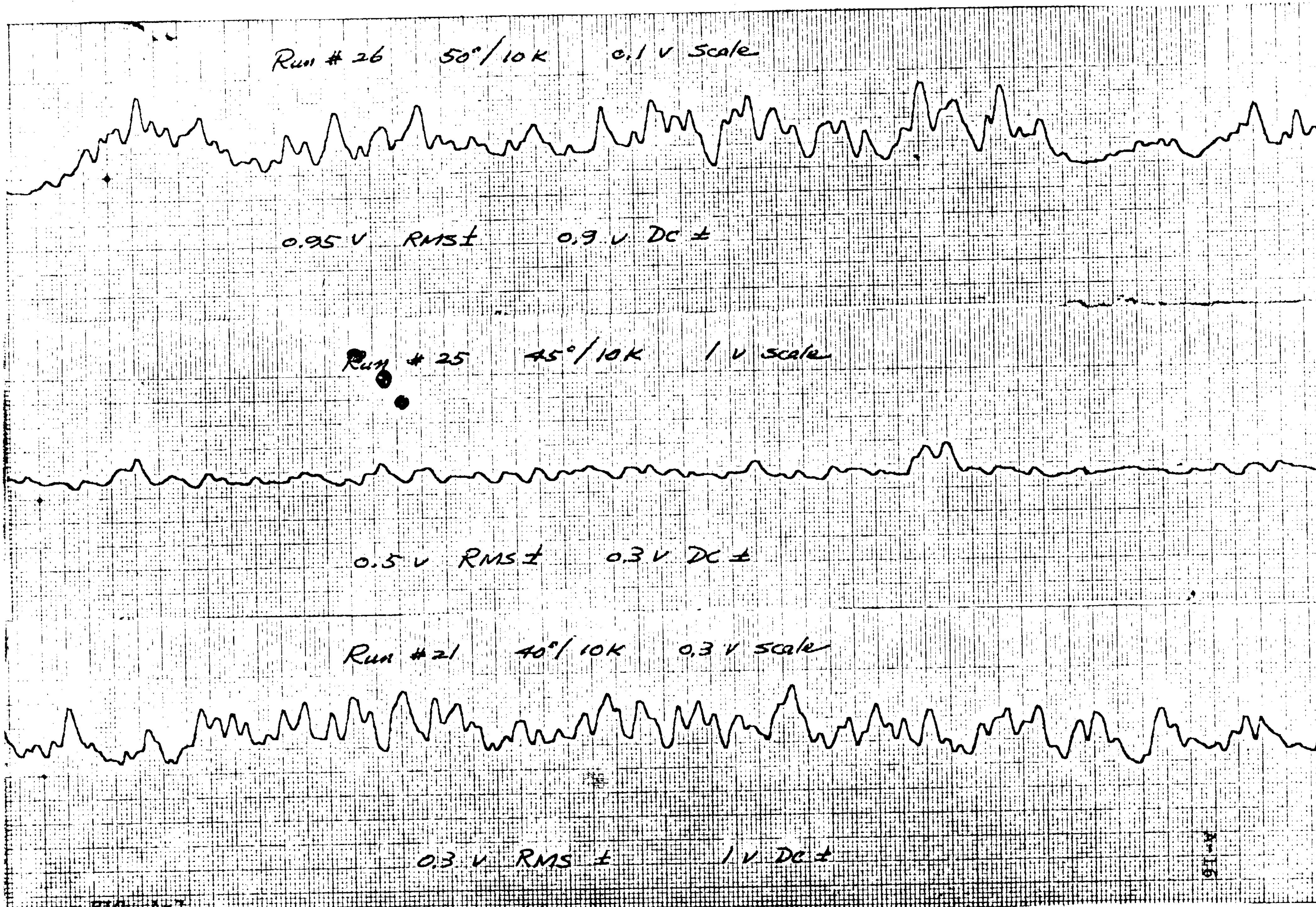

FIG. A-7.

AMPLITUDE DETECTOR OUTPUT OF SIMULATED RETURN FOR LUNAR SURFACE P-II-6 & 8 MODEL (Sheet 4 of 10)

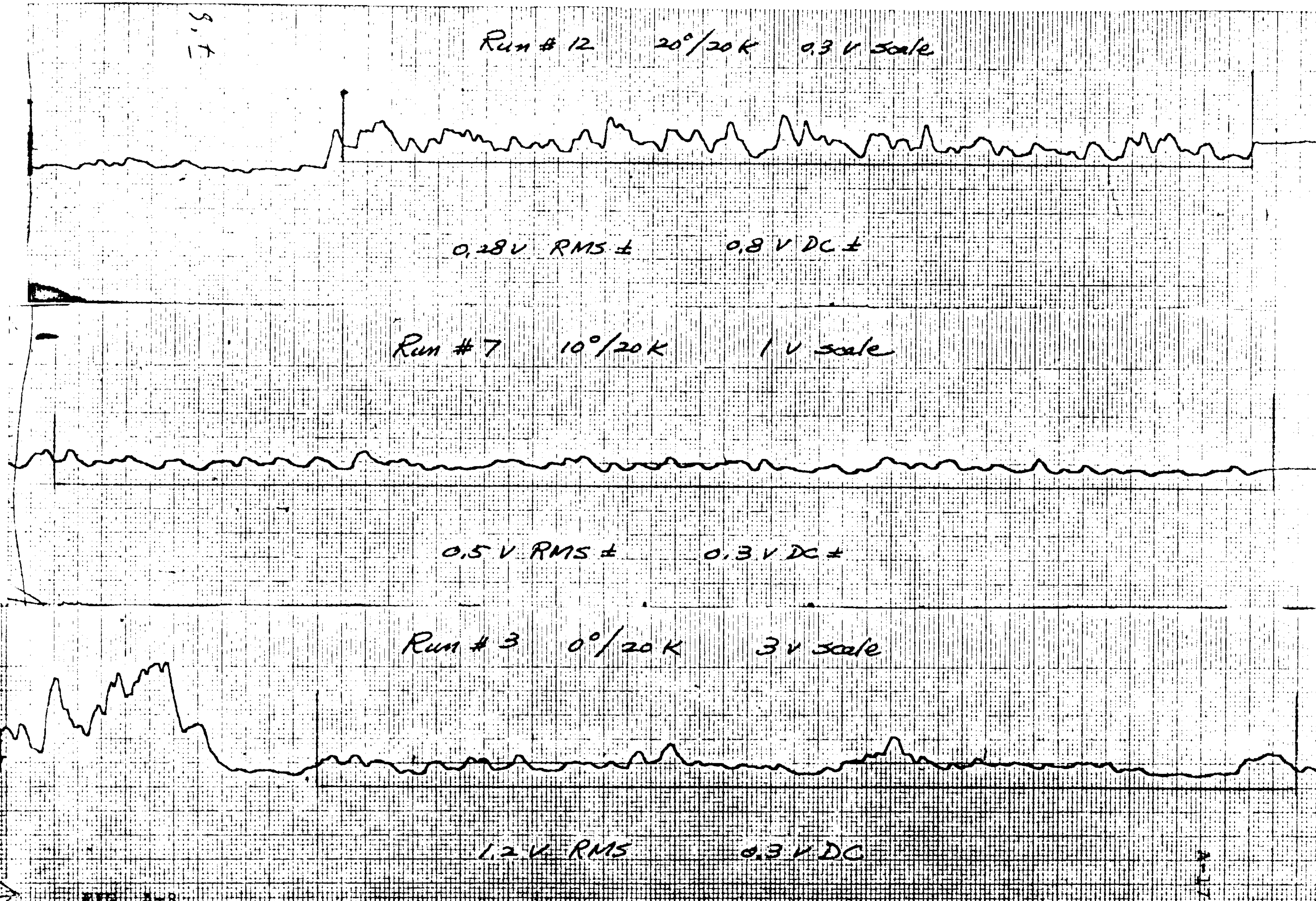

FIG. A-8
AMPLITUDE DETECTOR OUTPUT OF SIMULATED RETURN FOR LUNAR SURFACE P-II-6 & 8 MODEL (Sheet 5 of 10)

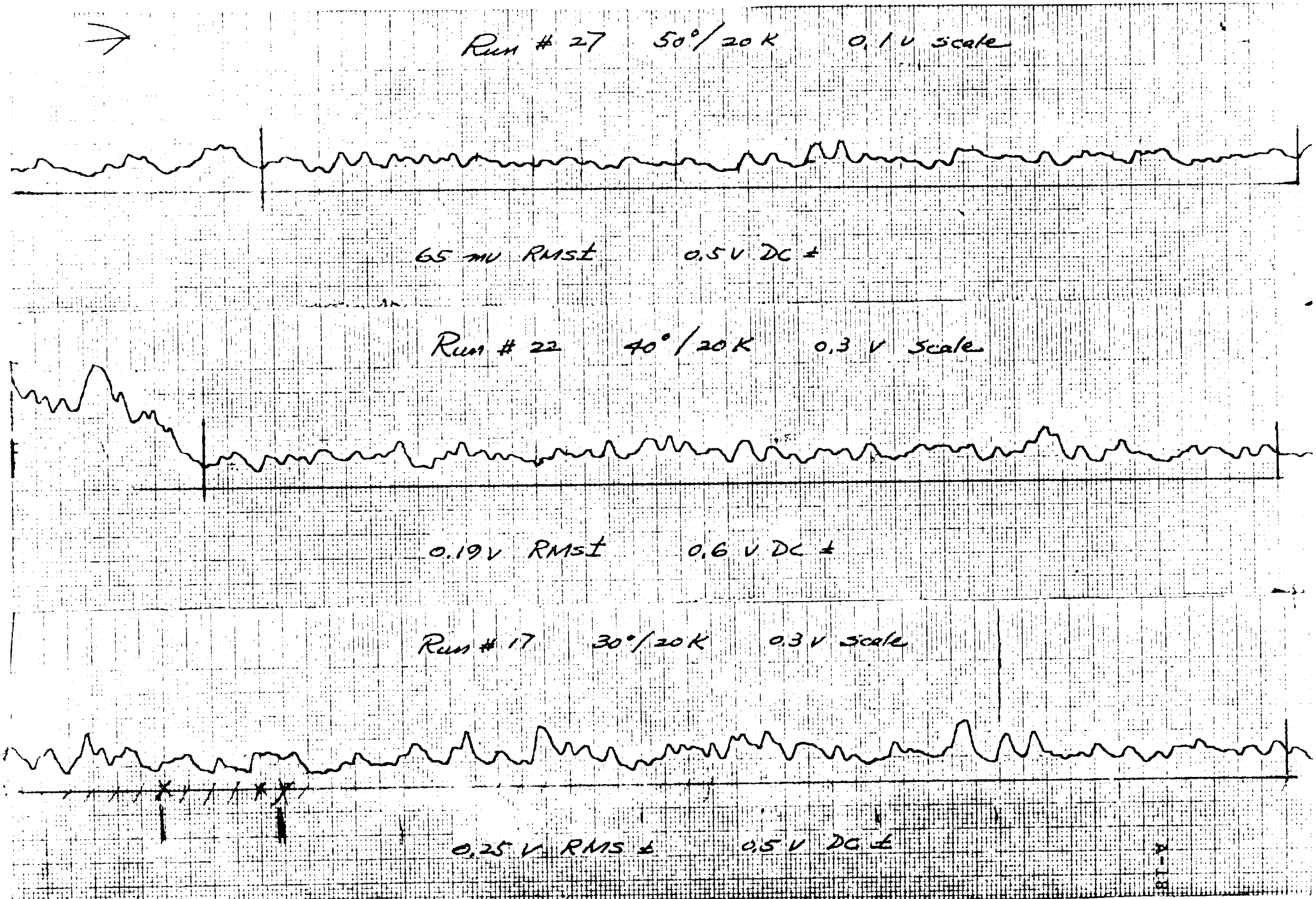

FIG. A-9
AMPLITUDE DETECTOR OUTPUT OF SIMULATED RETURN FOR LUNAR SURFACE P-II-6 & 8 MODEL (Sheet 6 of 10)

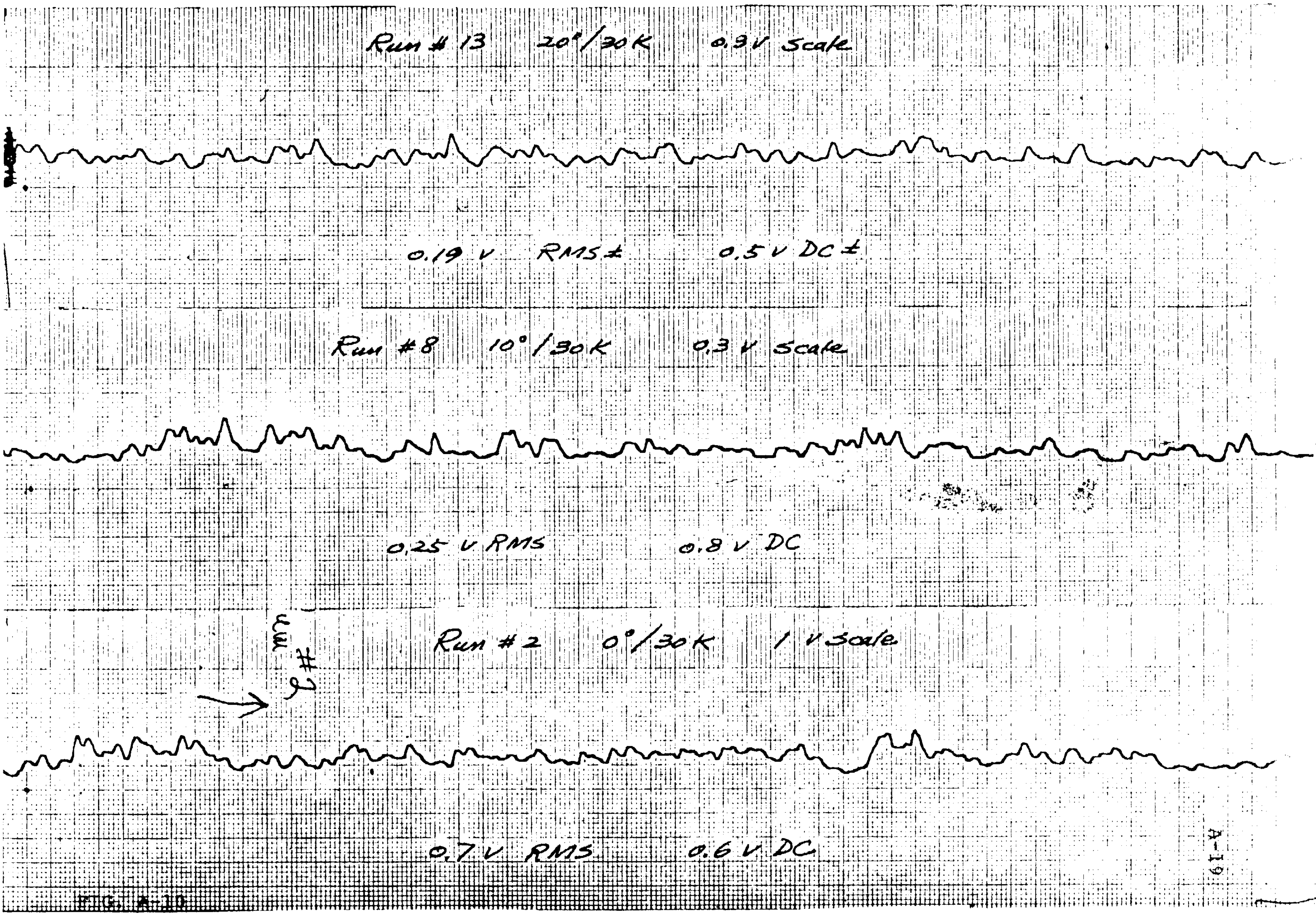

FIG. A-10

AMPLITUDE DETECTOR OUTPUT OF SIMULATED RETURN FOR LUNAR SURFACE P-II-6 & 8 MODEL (Sheet 7 of 10)

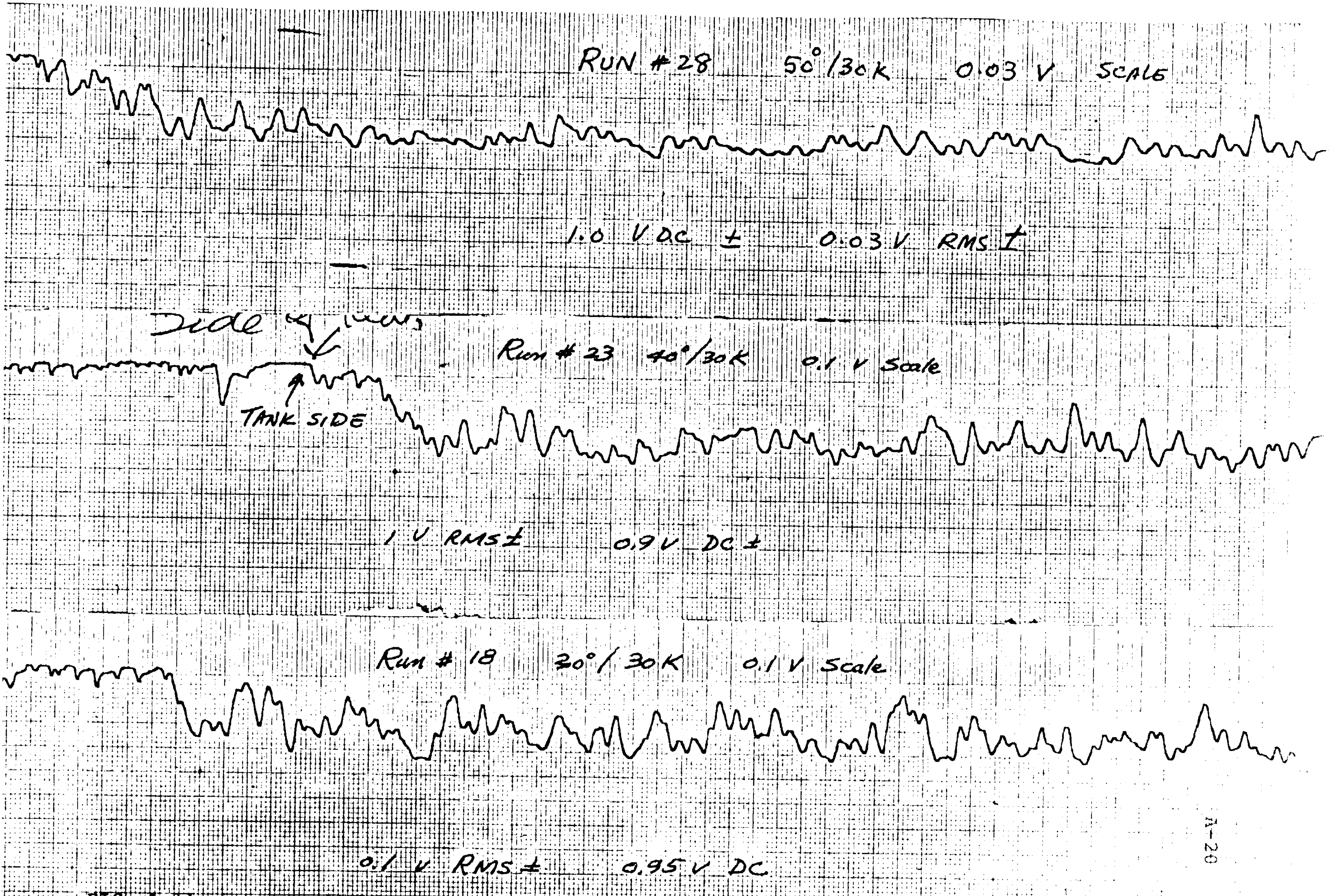

FIG. A-11
AMPLITUDE DETECTOR OUTPUT OF SIMULATED RETURN FOR LUNAR SURFACE P-II-6 & 8 MODEL

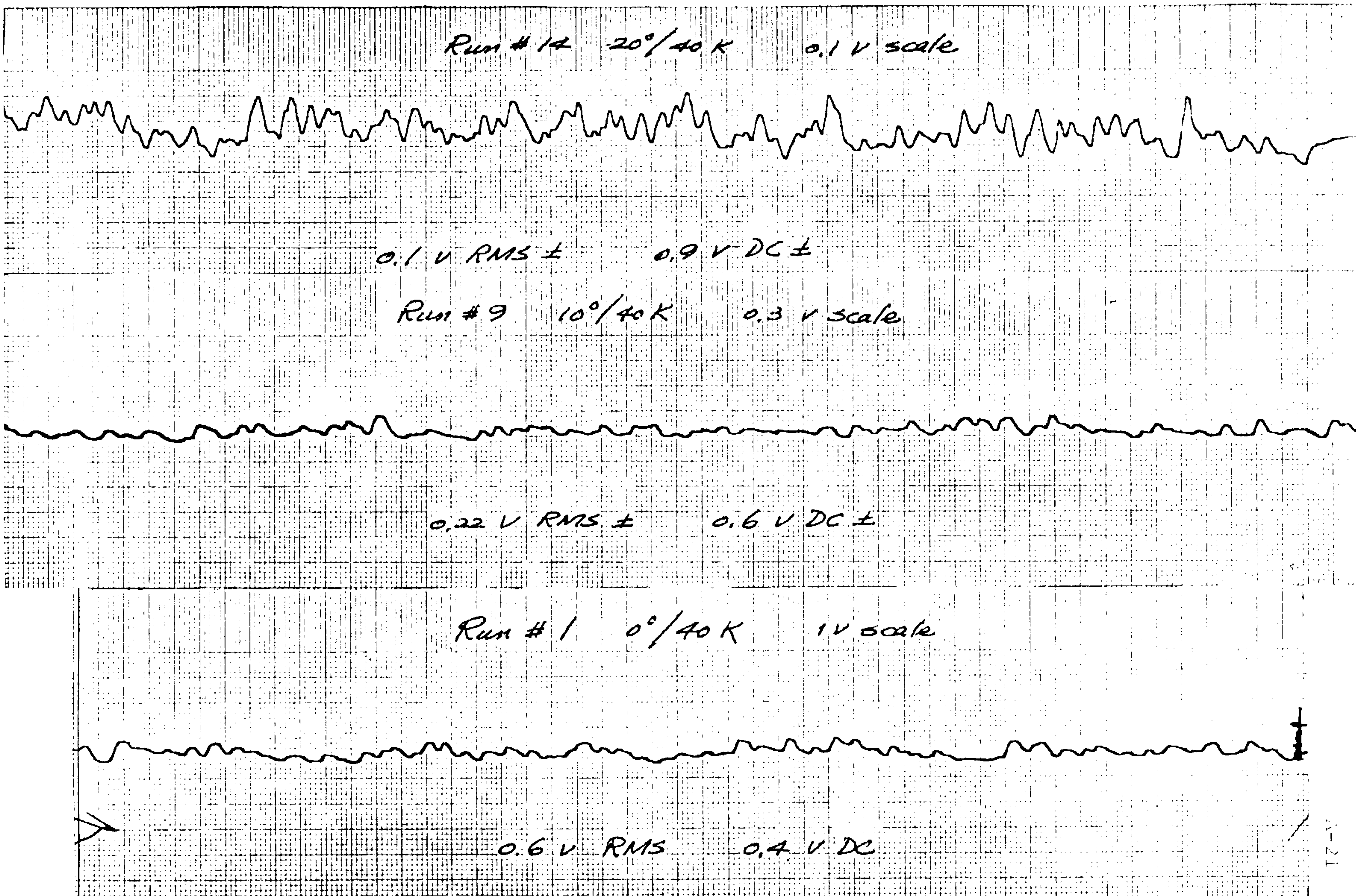

FIG. A-12
AMPLITUDE DETECTOR OUTPUT OF SIMULATED RETURN FOR LUNAR SURFACE P-II-6 & 8 MODEL (Sheet 9 of 10)

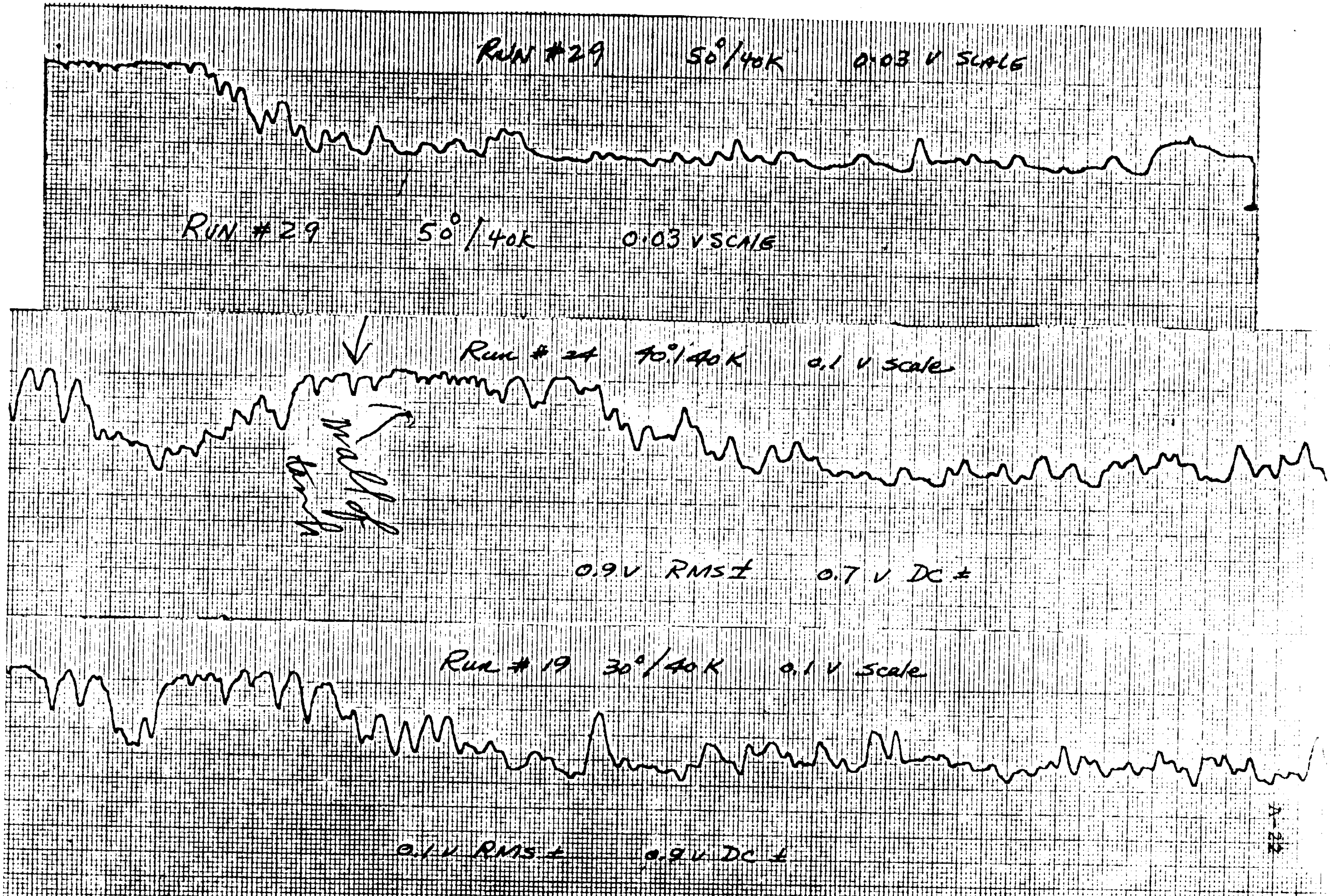

FIG. A-13
AMPLITUDE DETECTOR OUTPUT OF SIMULATED RETURN FOR LUNAR SURFACE P-II-6 & 8 MODEL (Sheet 10 of 10)

FIG. A-14 HUMMOCKS - WSMR TERRAIN FEATURES

(Top View)

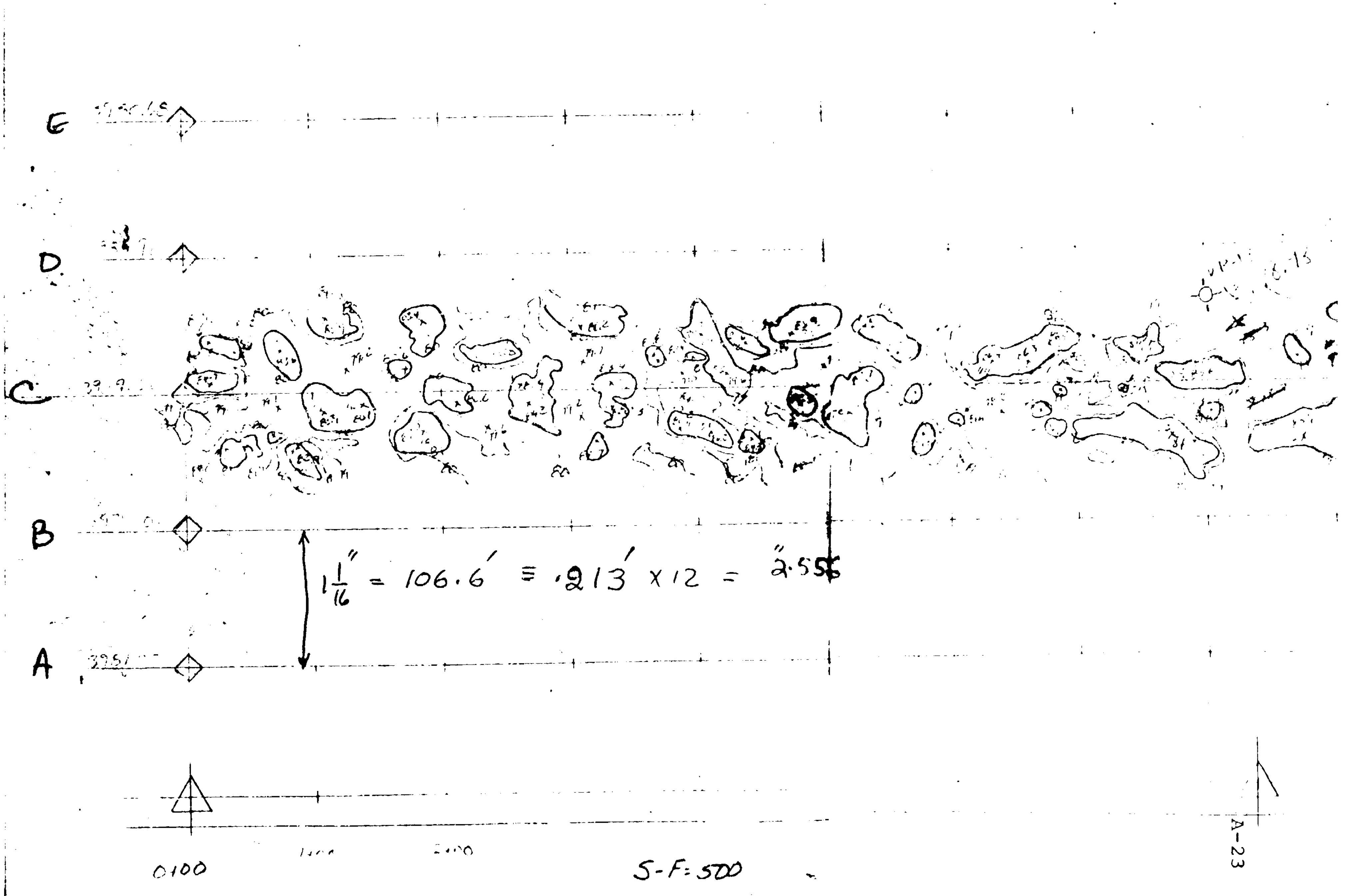

TABLE A-2

SUMMARY OF SIMULATED REFLECTIVITY DATA FOR HUMMOCKS - WSMR

Dist. (feet)	Run	Angle (degrees)	Actual voltage (volts) Mean m	Std. Dev σ	$m + \sigma$	$m - \sigma$	dB above 23.4 volts (Ref. 1K f.p. voltage) $m + \sigma$	m	$m - \sigma$
200	M	0°	5.91 (6.04)	3.32 (2.47)	9.23	2.69	- 8.08	-11.21	-18.8
300	N		4.84 (3.13)	2.61 (1.63)	7.45	2.23	- 9.94	-13.69	-20.40
400	O1		3.94 (3.14)	1.95 (1.67)	5.89	1.99	-12.00	-15.48	-21.40
500	O2		3.26 (3.30)	1.56	4.82	1.70	-13.73	-17.13 (-17.02)	-22.76
600	P		2.80 (2.70)	1.23 (1.29)	4.03	1.57	-15.28	-18.45 (-18.77)	-23.46
700	Q		2.50 (2.28)	1.00	3.50	1.50	-16.51	-19.43 (-20.23)	-23.86
800	R		2.19 (2.21)	0.77 (0.72)	2.96	1.42	-17.97	-20.56 (-20.50)	-24.34
900	S		2.02	0.64	2.66	1.38	-18.89	-21.28	-24.59
1000	T		1.89	0.54	2.43	1.35	-19.68	-21.85	-24.78

(Numbers in parentheses are values direct from calculatio

(Sheet 1 of 4)

TABLE A-2 (CONT'D)

SUMMARY OF SIMULATED REFLECTIVITY DATA FOR HUMMOCKS - WSMR

Dist. (feet)	Run	Angle (degrees)	Actual voltage (volts) Mean m	Std.Dev σ	$m + \sigma$	$m - \sigma$	dB above volts (Ref. K-f.p. voltage) $m + \sigma$	m	$m - \sigma$	(dB above 23.4 volts) (Ref. 1K-f.p. voltage) $m + \sigma$	m	$m - \sigma$
200	J	20°	2.53 (1.95)	1.28 (0.61)	3.81	1.25				-15.77	-19.33	-25.44
300	I		2.00 (1.14)	0.96 (0.41)	2.96	1.04				-17.96	-21.36	-27.04
400	H		1.64 (1.45)	0.72 (0.53)	2.36	0.92				-19.93	-23.08	-28.11
500	G2		1.36	0.55 (0.53)	1.91	0.81				-21.76	-24.71	-29.22
600	G1		1.15	0.425 (0.51)	1.57	0.73				-23.47	-26.16	-30.12
700	F		1.01 (1.02)	0.34	1.35	0.67				-24.76	-27.30 (-27.21)	-30.87
800	E		0.90 (0.91)	0.275 (0.26)	1.18	0.62				-25.94	-28.30 (-28.20)	-31.46
900	D		0.82	0.23	1.05	0.59				-26.96	-29.12	-31.98
1000	C		0.775 (0.74)	0.20	0.98	0.58				-27.56	-29.60 (-30.00)	-32.12

(Numbers in parentheses are values direct from calculation

(Sheet 2 of 4)

TABLE A-2 (CONT'D)

SUMMARY OF SIMULATED REFLECTIVITY DATA FOR HUMMOCKS - WSMR

Recorded Information					From Equation		True	Ref. Scale to 1 V.		Convert to voltage		No. of
Angle/ Dist.	V. M. Scale	Read. Ref.	ΣX	ΣX^2	m	σ	Mean	m	σ	m	σ	Read.
0/200	3	30mm	2040.2	20392.04	6.581	4.748	11.581	36.60	15.0	6.04	2.47	310
0/300	3	25	1764.5	13445.25	6.00	3.121	6.00	19.0	9.00	3.135	1.63	294
0/400	3	25	1810.5	14014.75	6.035	3.214	6.03	19.05	10.15	3.14	1.674	300
0/500	3	25	1937.1	14976.13	6.33	2.983	6.33	20.0	9.45	3.3	1.56	306
0/600	3	25	1628.5	10360.25	5.17	2.486	5.17	16.35	7.857	2.7	1.296	315
0/700	3	25	1351	7026.0	4.358	1.919	4.36	13.8	6.06	2.28	1.00	311
0/800	1	35	954	8604.5	3.407	4.380	13.41	13.41	4.38	2.21	0.722	280
0/900	1	35	692.5	6077.25	2.27	3.849	12.27	12.27	3.85	2.02	0.635	305
0/1000	1	30	1993.5	16108.5	6.43	3.27	11.43	11.43	3.27	1.89	0.54	310

Anti $\log_{10}$ 0.5=3.16 Scale $\frac{4.283}{26} = 0.165$

(Sheet 3 of 4)

TABLE A-2 (CONT'D)

SUMMARY OF SIMULATED REFLECTIVITY DATA FOR HUMMOCKS - WSMR

Recorded Information					From Equation		True	Ref. Scale to 1 V.		Convert to voltage		No. of
Angle/ Dist.	V. M. Scale	Read. Ref.	ΣX	ΣX^2	m	σ	Mean	m	σ	m	σ	Read.
20/200	1	30	1880.5	16668.25	6.838	3.728	11.838	11.838	3.728	1.954	0.615	275
20/300	1	25	1867.9	14570.11	6.892	2.505	6.892	6.892	2.505	1.137	0.413	271
20/400	1	30	1008.0	6538.0	3.804	3.20	8.804	8.804	3.20	1.452	0.528	265
20/500	1	30	903.5	5820.75	3.227	3.227	8.227	8.227	3.227	1.357	0.532	280
20/600	1	25	1916.5	16000.25	6.969	3.106	6.969	6.969	3.106	1.15	0.512	275
20/700	1	30	348	1616.0	1.2	2.036	6.20	6.20	2.036	1.023	0.336	290
20/800	1	25	1519.0	9093.50	5.523	1.602	5.523	5.523	1.602	0.911	0.264	275
20/900	0.3	35	1530.0	14010.5	5.773	4.428	15.773	4.984	1.399	0.822	0.231	265
20/1000	0.3	35	1187	9112	4.16	3.835	14.16	4.47	1.21	0.74	0.20	285

(Sheet 4 of 4)

TABLE A-3

BASE AND TOP HEIGHTS OF HUMMOCKS (WSMR) CENTER STRIP

BASE	TOP	HEIGHT	BASE	TOP	HEIGHT	BASE	TOP	HEIGHT
80	82.9	2.9	82	86.4	4.4	80	86.5	6.5
80	82.2	2.2	82	86.2	4.2	80	83.6	3.6
81	84.7	3.7	82	84.3	2.3	81	84.7	3.7
81	84.2	3.2	79	79.6	.6	80	81.8	1.8
80	81.9	1.9	82	85.6	3.6	79	81.9	2.9
80	83.6	3.6	82	85.9	3.9	79	83.9	4.9
80	82.9	2.9	80	82.5	2.5	79	84.8	5.8
80	85.9	5.9	80	87.0	7.0	79	79.5	.5
80	83.1	3.1	80	83.7	3.7	78	81	3.0
80	82.6	2.6	81	84.8	3.8	79	82.6	3.6
81	87.3	6.3	81	85.5	4.5	80	82.1	2.1
80	82.6	2.6	80	80.6	.6	78	81	3.0
81	84.9	3.9	81	84.0	3.0	77	78.5	1.5
80	82.9	2.9	81	81.9	.9	77	78.5	1.5
80	84.2	4.2	82	86.4	4.4	78	80.3	2.3
81	81.7	.7	82	86.3	4.3	78	81.8	3.8
81	82.3	1.3	82	86.5	4.5	78	85	7.0
81	83.4	2.4	79	79.6	.6	78	80.1	2.1
81	86.2	5.2	79	80.1	.1	78	82.2	4.2
81	82.8	1.8	79	80.3	1.3	78	81.7	4.7
80	82.4	2.4	81	81.4	.4	77	77.7	.7

TABLE A-3 (CONT'D)

BASE	TOP	HEIGHT	BASE	TOP	HEIGHT	BASE	TOP	HEIGHT
77	79.9	2.9	73	78.8	5.8	71	72.6	1.6
78	78.1	.1	74	77.0	3.0	71	80.5	9.5
77	83.8	6.8	73	75.4	2.4	71	76.4	5.4
77	78.5	1.5	73	75.6	2.6	72	75.3	3.3
76	78.4	2.4	74	79.6	5.6	72	75.4	3.4
77	80.6	3.6	74	79.3	5.3	72	73.9	1.9
77	79.1	2.1	74	77.9	3.9	73	78.2	5.2
76	83	7.0	74	95.7	21.7	73	75.2	2.2
76	78.4	2.4	73	78.1	5.1	73	76.9	3.9
75	78.6	3.6	72	76.5	4.5	73	74.8	1.8
75	78.4	3.4	73	75.1	2.1	74	75.6	2.6
75	80.2	5.2	73	76.9	3.9	72	75.3	3.3
75	81.3	6.3	72	81.1	9.1	72	76.5	4.5
75	78.4	3.4	72	74.8	2.8	72	74.6	2.6
74	76.4	2.4	72	74.3	2.3	73	74.4	1.4
75	78.1	3.1	71	76.9	5.9	73	75.3	2.3
75	80.1	5.1	71	80.5	9.5	74	77.4	3.4
74	76.6	2.6	71	76.1	5.1	74	82.3	8.3
74	79.3	4.3	71	75.1	4.1	74	77.5	3.5
75	81.5	6.5	71	75.0	4.0	75	81.4	6.4
74	77.0	3.0	71	79.0	8.0	74	78.2	4.2
74	77.4	3.4	71	76.8	5.8	74	75.6	1.6
73	80.4	7.4	71	77.8	6.8	75	81.4	6.4
73	75.1	2.1	71	78.7	7.7	76	78.8	2.8

TABLE A-3 (CONT'D)

BASE	TOP	HEIGHT	BASE	TOP	HEIGHT	BASE	TOP	HEIGHT
75	77.4	2.4	73	74.3	1.3	72	73.7	1.7
75	76.3	1.3	72	73.7	1.7	71	73.2	2.2
75	76.9	1.9	72	74.0	2.0	71	73.4	2.4
75	76.9	1.9	72	73.3	1.3	71	76.7	5.7
75	76.6	1.6	72	73.2	1.2	71	73.2	2.2
75	78.4	3.4	72	75.8	3.8	71	77.6	6.6
75	77.1	2.1	72	74.5	2.5	72	74.5	2.5
74	76.7	2.7	71	75.0	4.0	71	72.9	1.9
76	79.9	3.9	71	74.3	3.3	72	74.2	2.2
74	78.6	4.6	71	72.9	1.9	71	73.1	2.1
74	75.8	1.8	70	71.5	1.5	71	72.6	1.6
73	75.5	2.5	71	74.7	3.7	71	76.2	5.2
75	80.0	5.0	70	71.5	1.5	71	73.5	2.5
75	76.5	1.5	70	71.6	1.6	71	74.0	3.0
75	75.3	.3	71	74.8	3.8	71	72.1	1.1
73	76.3	3.3	72	73.1	1.1	71	71.7	.7
73	74.6	1.6	71	72.1	1.1	71	75.7	4.7
73	75.0	2.0	71	73.6	2.6	71	72.8	1.8
73	75.0	2.0	71	73.5	2.5	72	74.0	2.0
74	77.5	3.5	72	76.3	4.3	72	74.4	2.4
73	74.9	1.9	71	72.8	1.8	71	73.3	2.3
72	74.4	2.4	71	73.0	2.0	71	74.0	3.0
73	75.1	2.1	72	73.7	1.7	72	73.3	1.3

TABLE A-3 (CONT'D)

BASE	TOP	HEIGHT
72	74.1	2.1
72	76.5	4.5
72	73.2	1.2
72	75.0	3.0
71	73.8	2.8
71	74.0	3.0
71	73.6	2.6
72	75.3	3.3
71	72.2	1.2
71	73.4	2.4
71	74.3	3.3
71	72.5	1.5
71	72.4	1.4
71	77.4	6.4
71	74.3	3.3
71	74.2	3.2
72	72.9	.9
71	73.3	2.3
71	72.3	1.3
71	72.3	1.3
72	74.7	2.7
72	76.4	4.4
71	77.0	6.0

BASE	TOP	HEIGHT
71	72.8	1.8
72	74.1	2.1
72	75.5	3.5
72	76.8	4.8
72	76.1	4.1
72	78.0	6.0
72	79.2	7.2
71	73.6	2.6
71	74.0	3.0
71	72.6	1.6
72	77.6	5.6
71	77.0	6.0
71	75.0	4.0

Horizontal Scale 1"=500'
Vertical Scale 1"=10'

Profile A

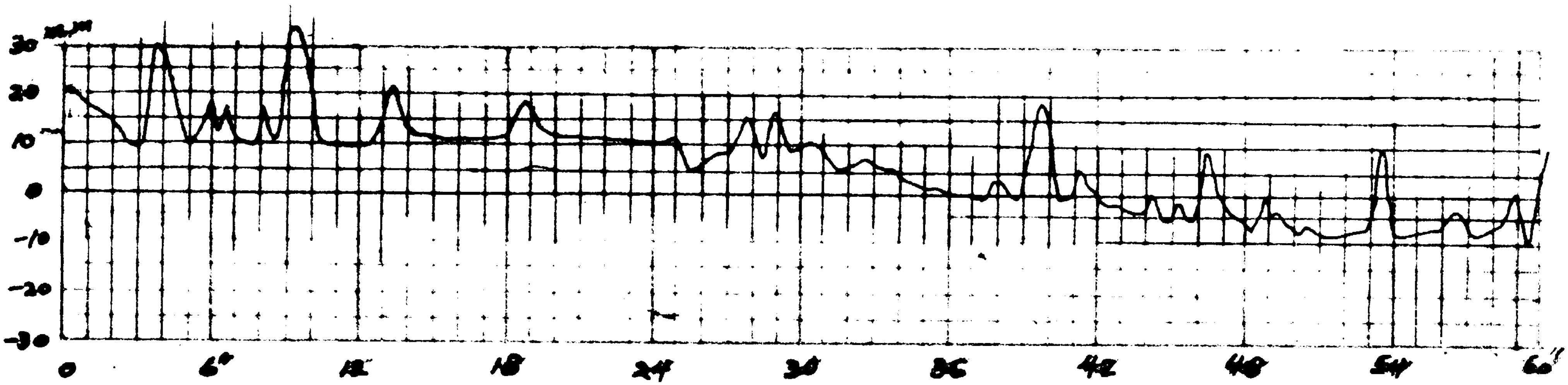

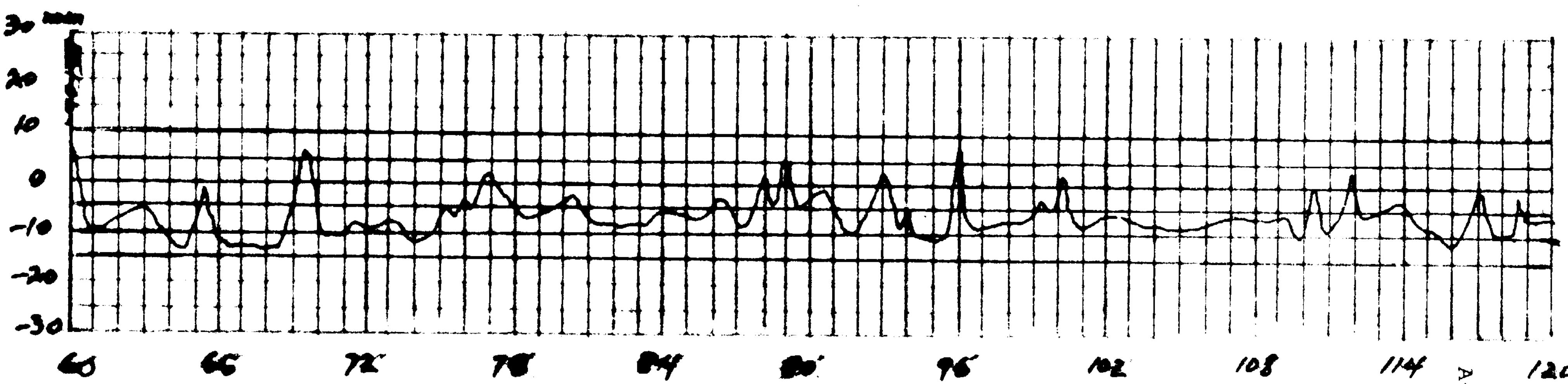

FIG. A-15 TERRAIN PROFILE--HUMMOCKS AREA--WSMR

Horizontal Scale 1"=500'
Vertical Scale 1"=10'

Profile B

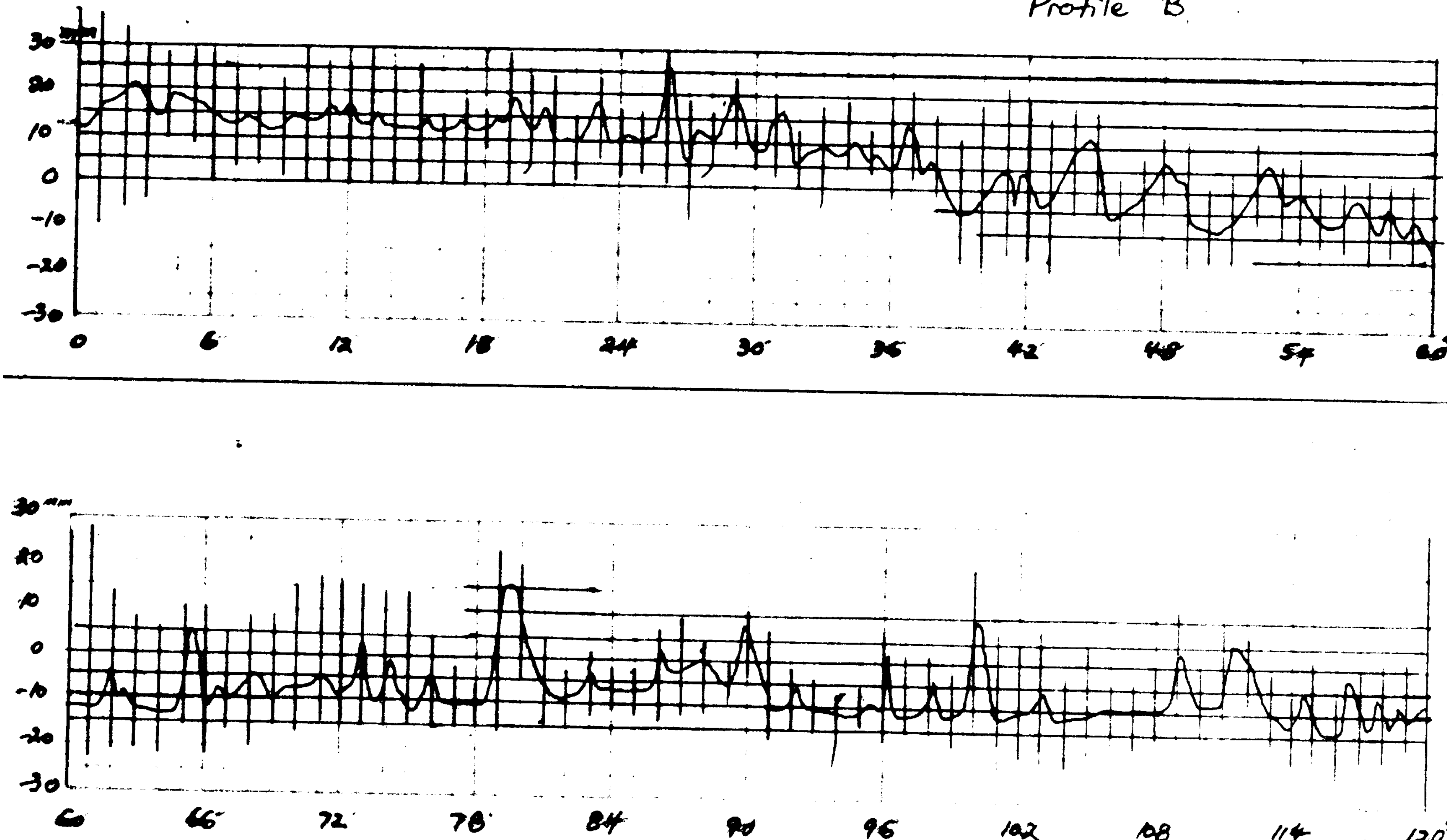

FIG. A-16. TERRAIN PROFILE--HUMMOCKS AREA--WSMR

Horizontal Scale 1"=500'
Vertical Scale 1"=10'

Profile D

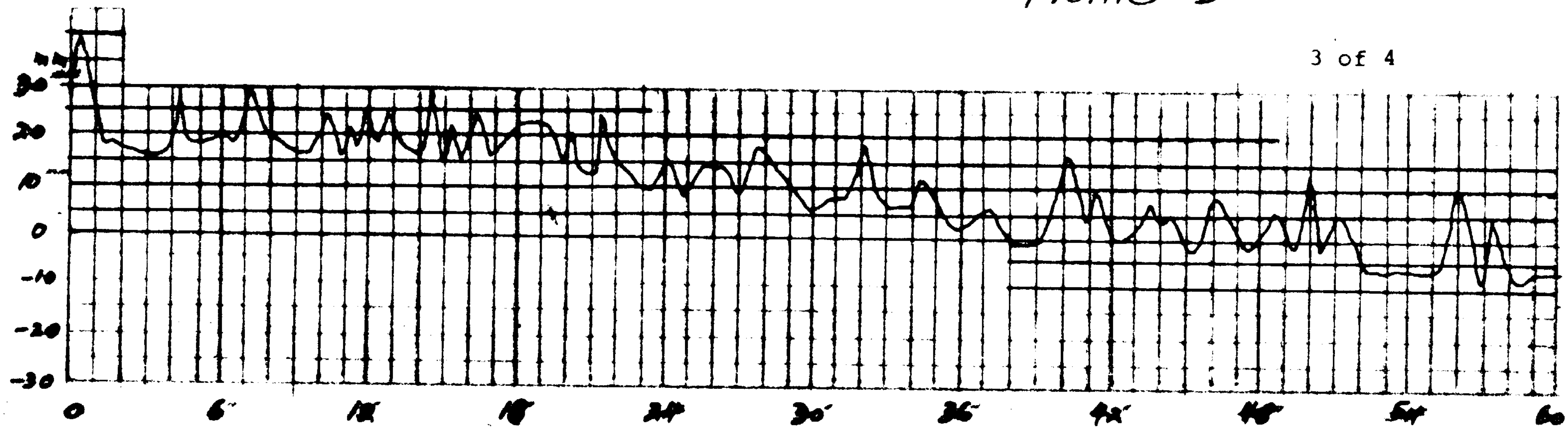

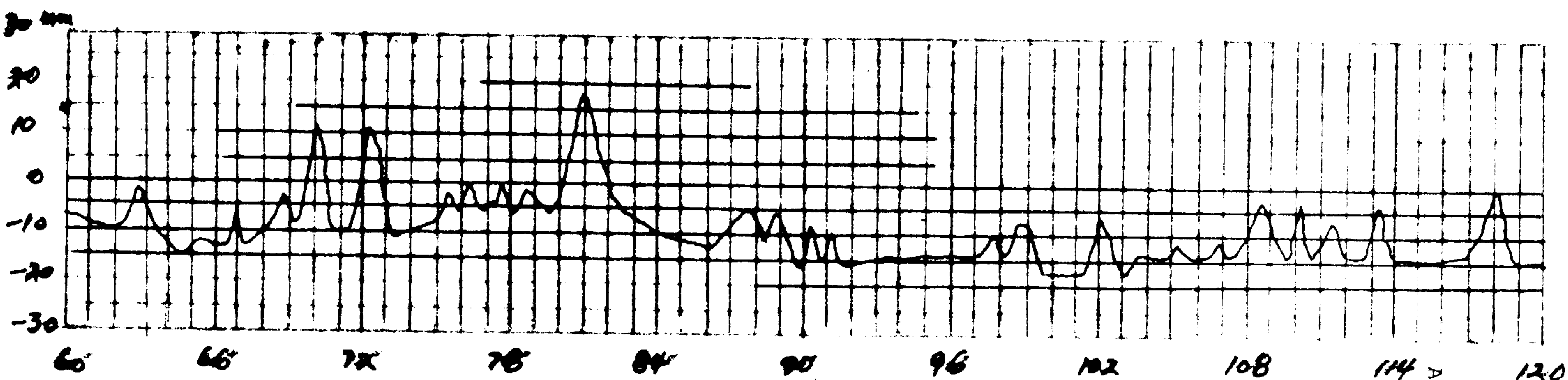

FIG. A-17. TERRAIN PROFILE--HUMMOCKS AREA--WSMR

Horizontal Scale 1"=500'
Vertical Scale 1"=10'

Profile E

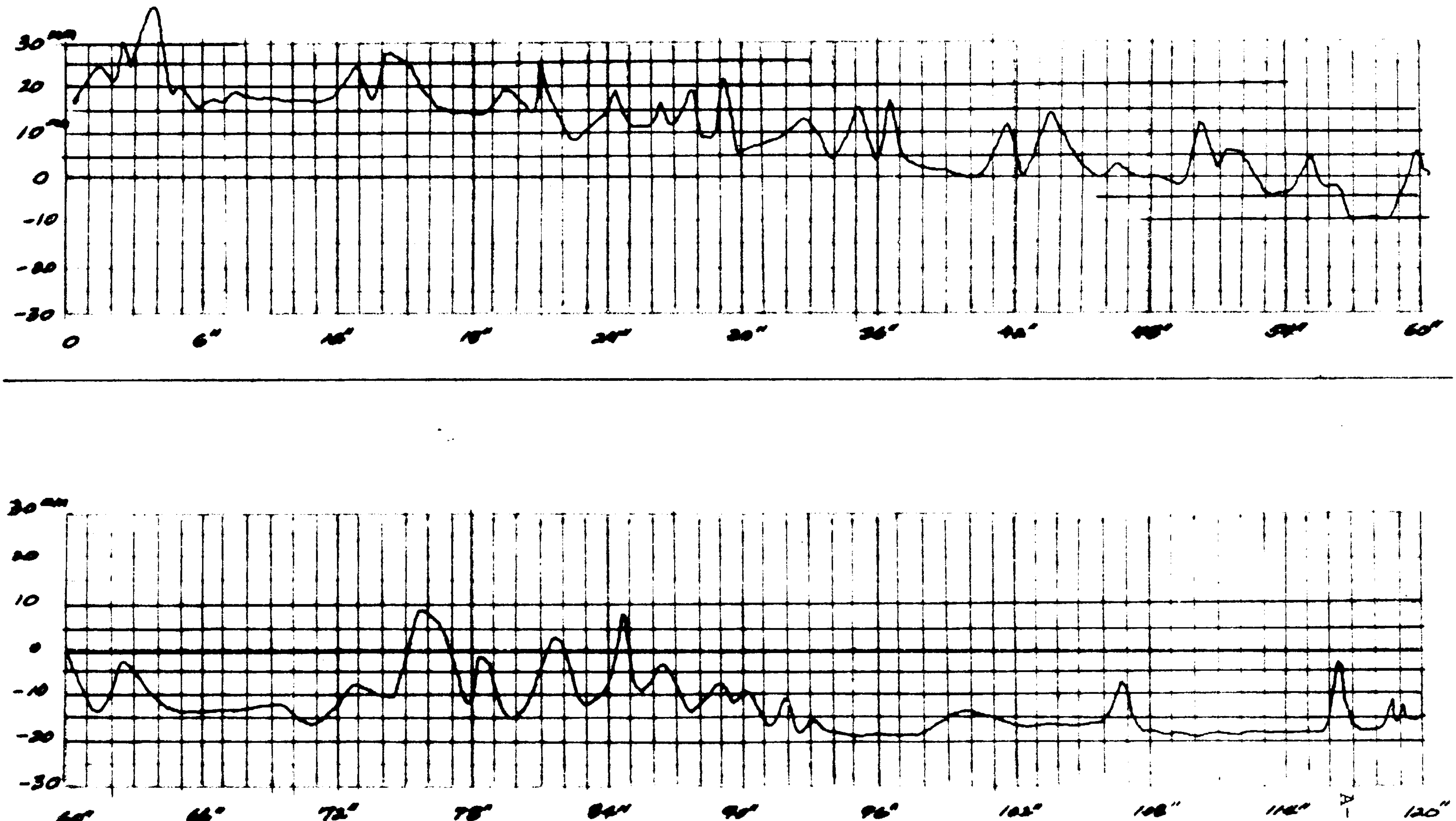

FIG. A-18. TERRAIN PROFILE--HUMMOCKS AREA--WSMR

FIG. A-19 S[illegible]TED DATA VERSUS ALTITUDE FOR 0 [illegible]
INCIDENCE ANGLES FOR HUMMOCKS - WSM[illegible]

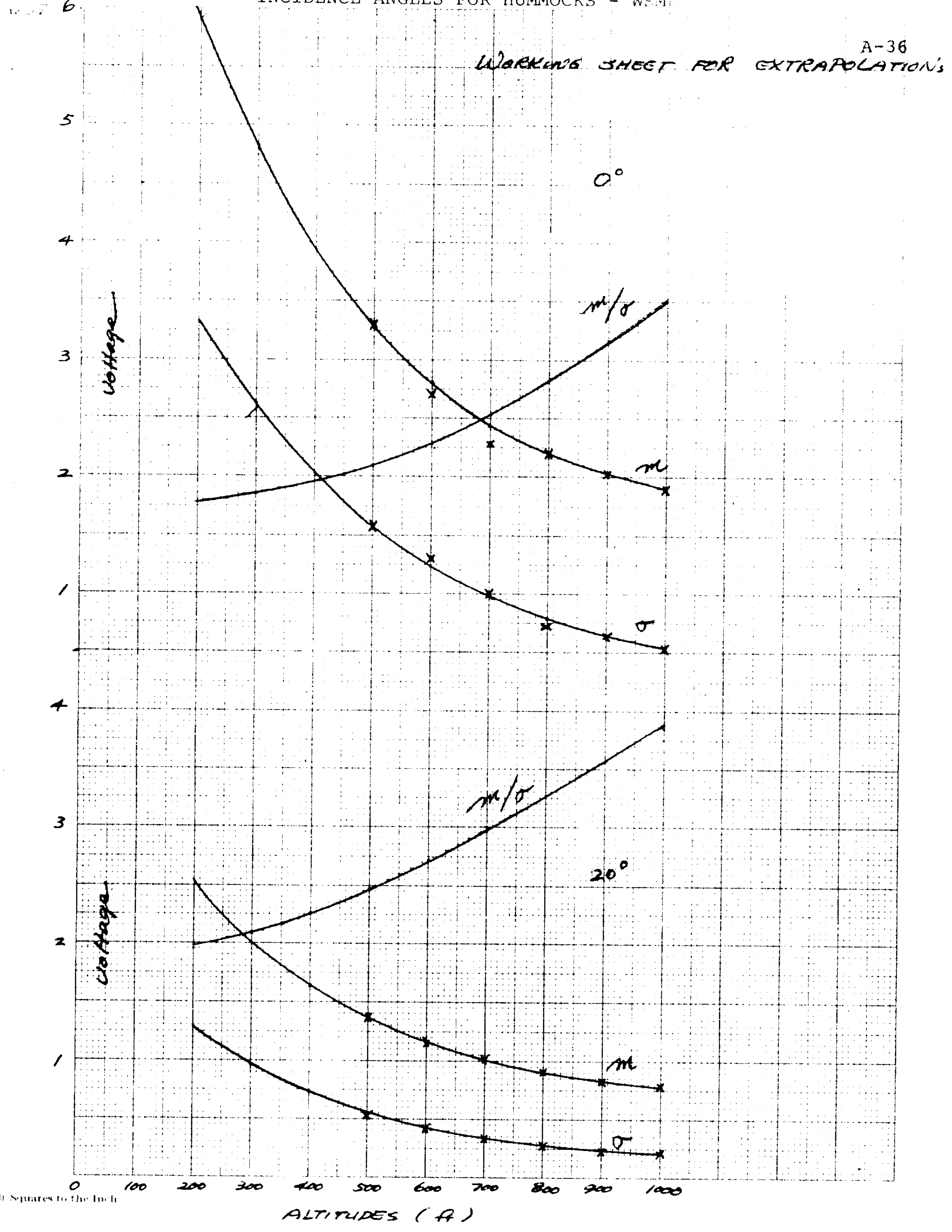

10 Squares to the Inch

INCIDENCE ANGLES FOR ...

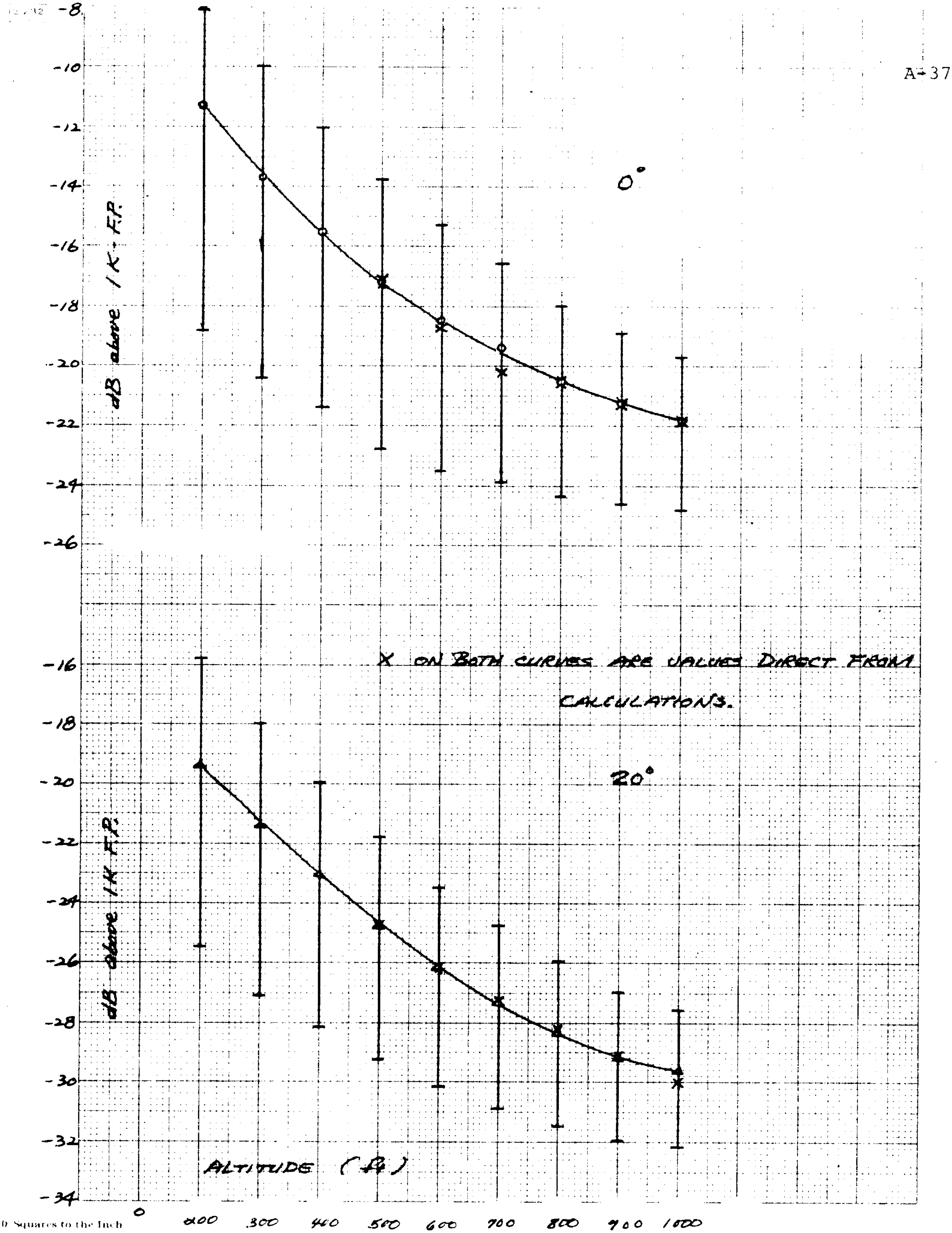

0 Squares to the Inch

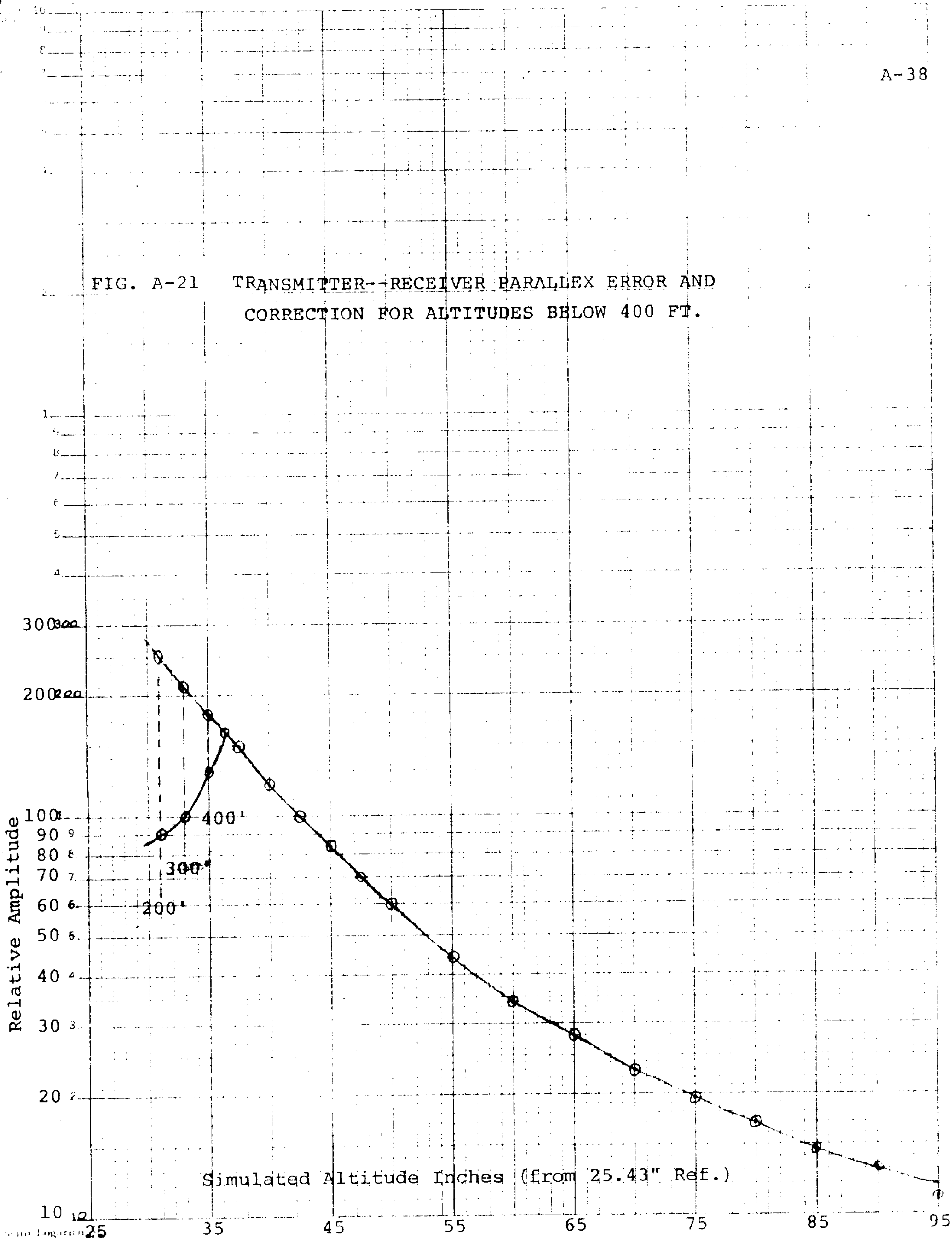

FIG. A-21 TRANSMITTER--RECEIVER PARALLEX ERROR AND CORRECTION FOR ALTITUDES BELOW 400 FT.

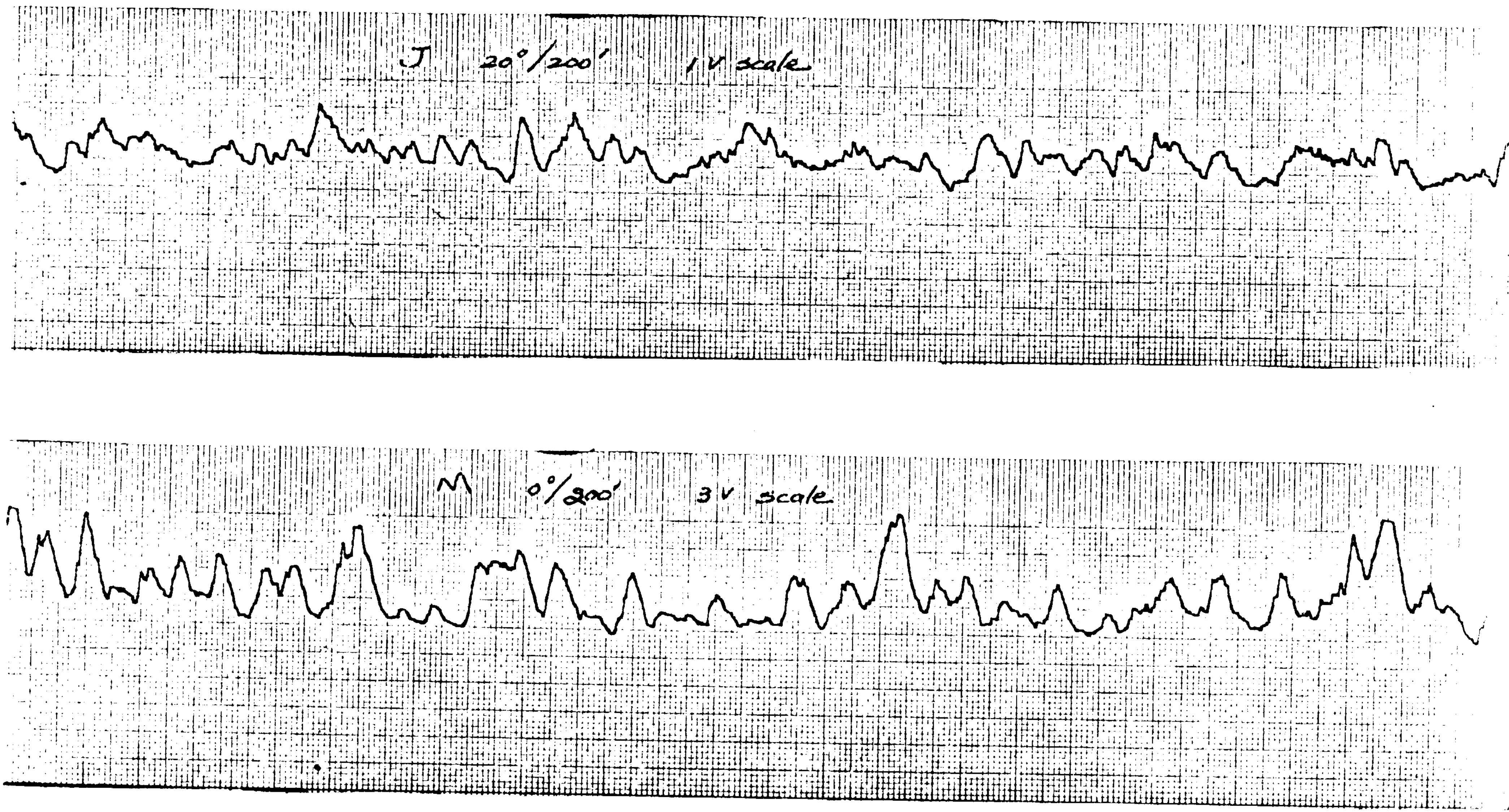

FIG. A-22 AMPLITUDE DETECTOR OUTPUT OF SIMULATED RETURN FOR HUMMOCKS - WSMR
(Sheet 1 of 9)

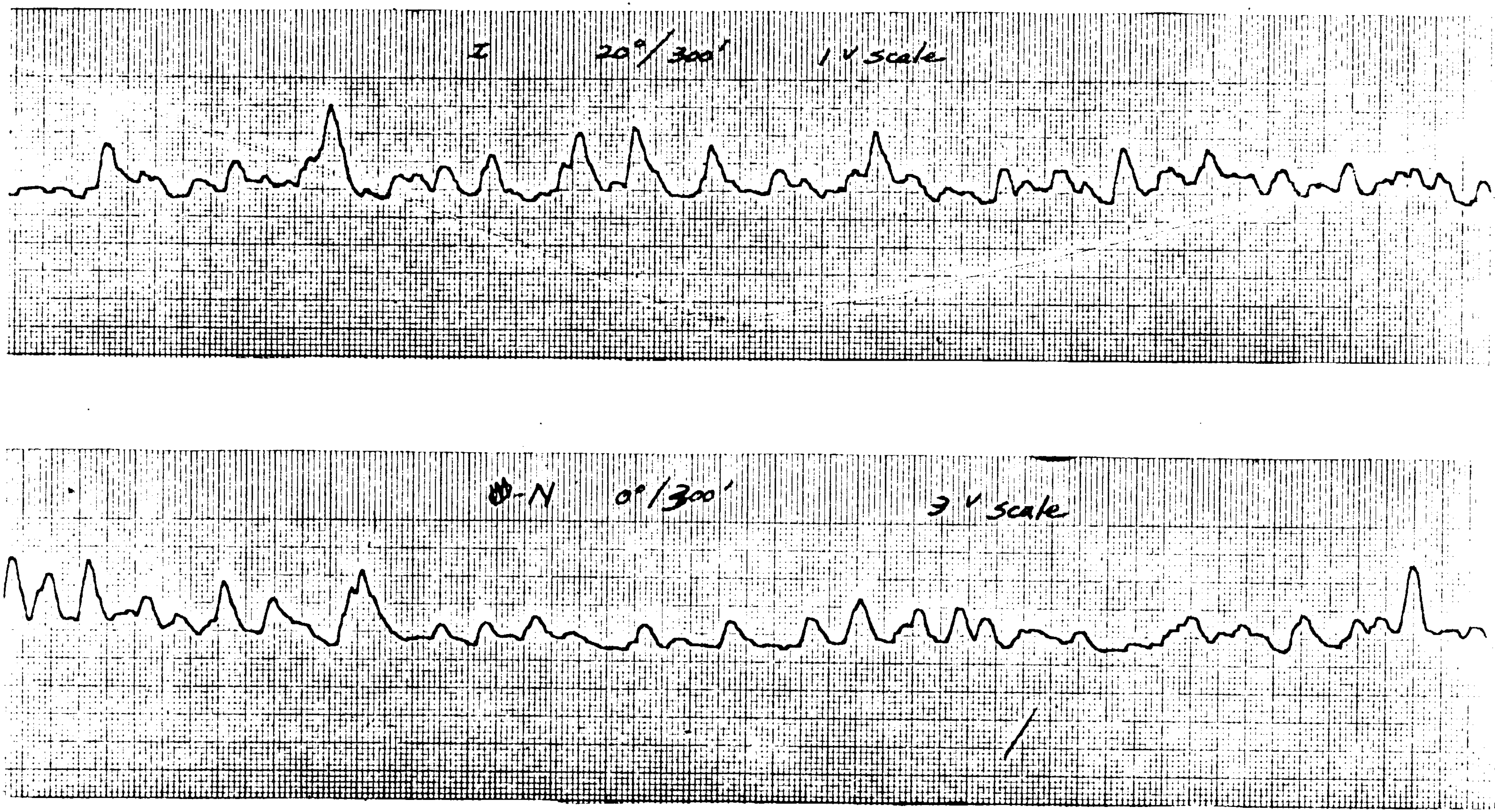

FIG. A-23 AMPLITUDE DETECTOR OUTPUT OF SIMULATED RETURN FOR HUMMOCKS - WSMR
(Sheet 2 of 9)

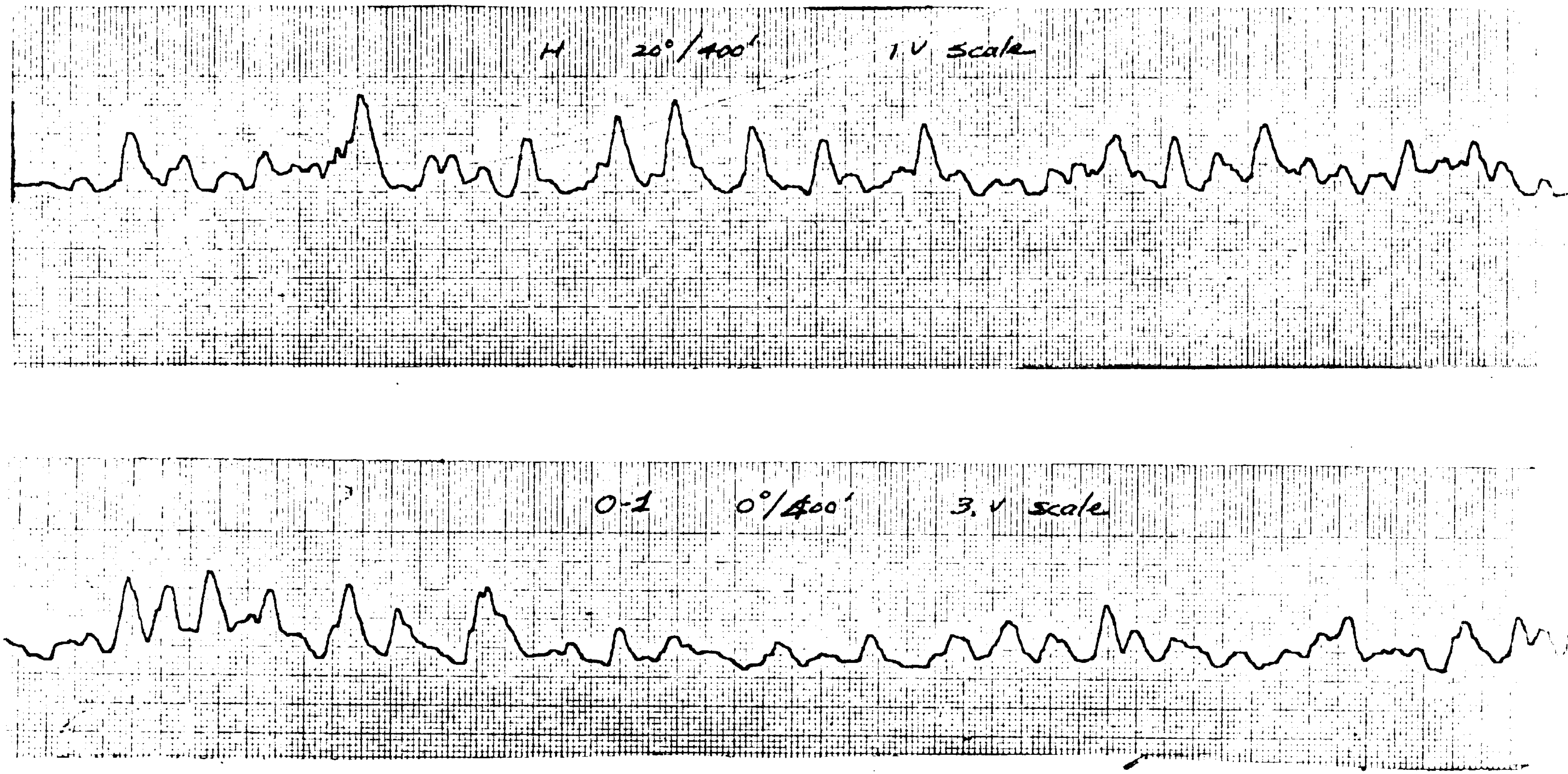

FIG. A-24 AMPLITUDE DETECTOR OUTPUT OF SIMULATED RETURN FOR HUMMOCKS - WSMR
(Sheet 3 of 9)

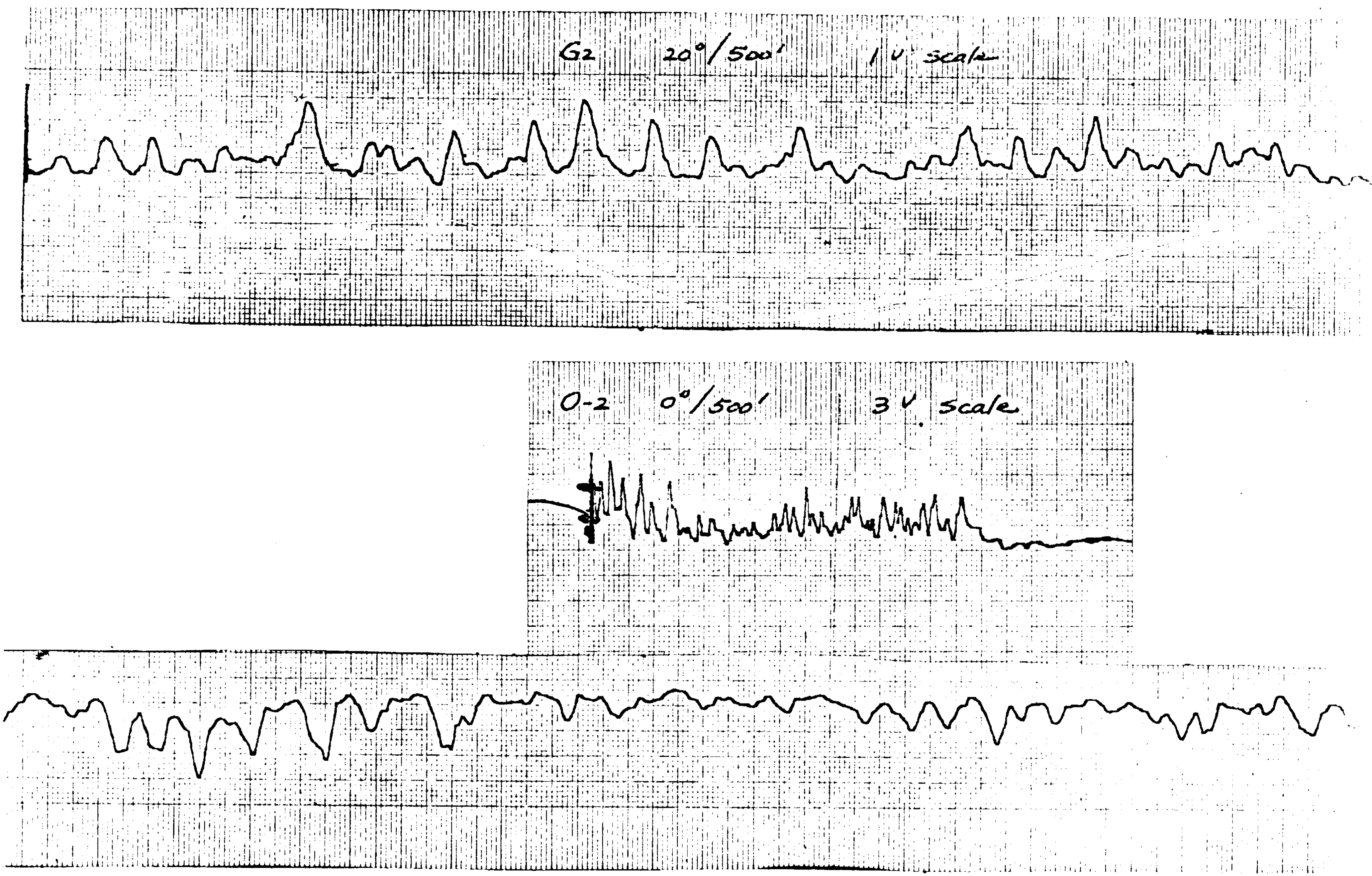

FIG. A-25 AMPLITUDE DETECTOR OUTPUT OF SIMULATED RETURN FOR HUMMOCKS - WSMR
(Sheet 4 of 9)

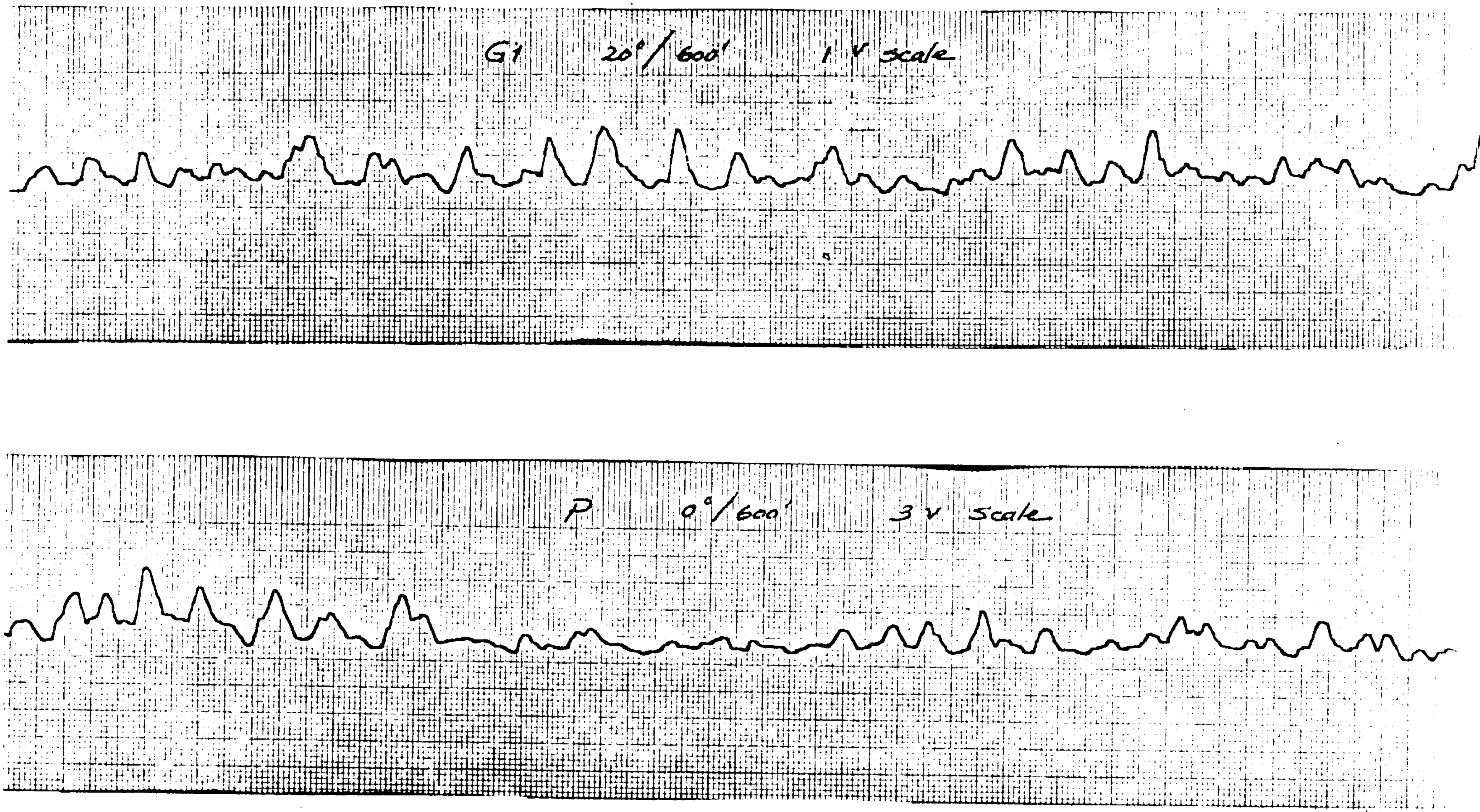

FIG. A-26 AMPLITUDE DETECTOR OUTPUT OF SIMULATED RETURN FOR HUMMOCKS - WSMR
(Sheet 5 of 9)

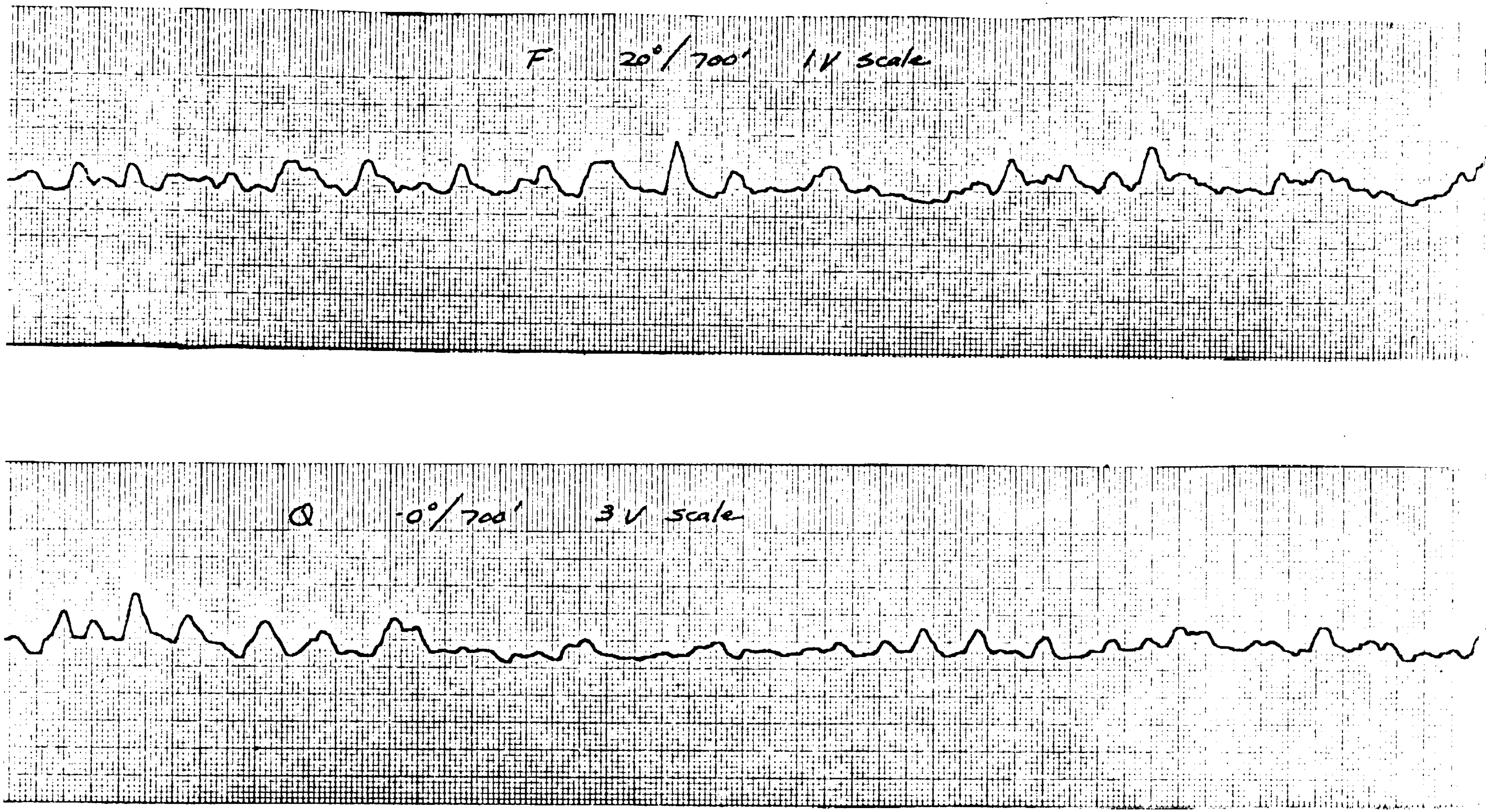

FIG. A-27 AMPLITUDE DETECTOR OUTPUT OF SIMULATED RETURN FOR HUMMOCKS - WSMR
(Sheet 6 of 9)

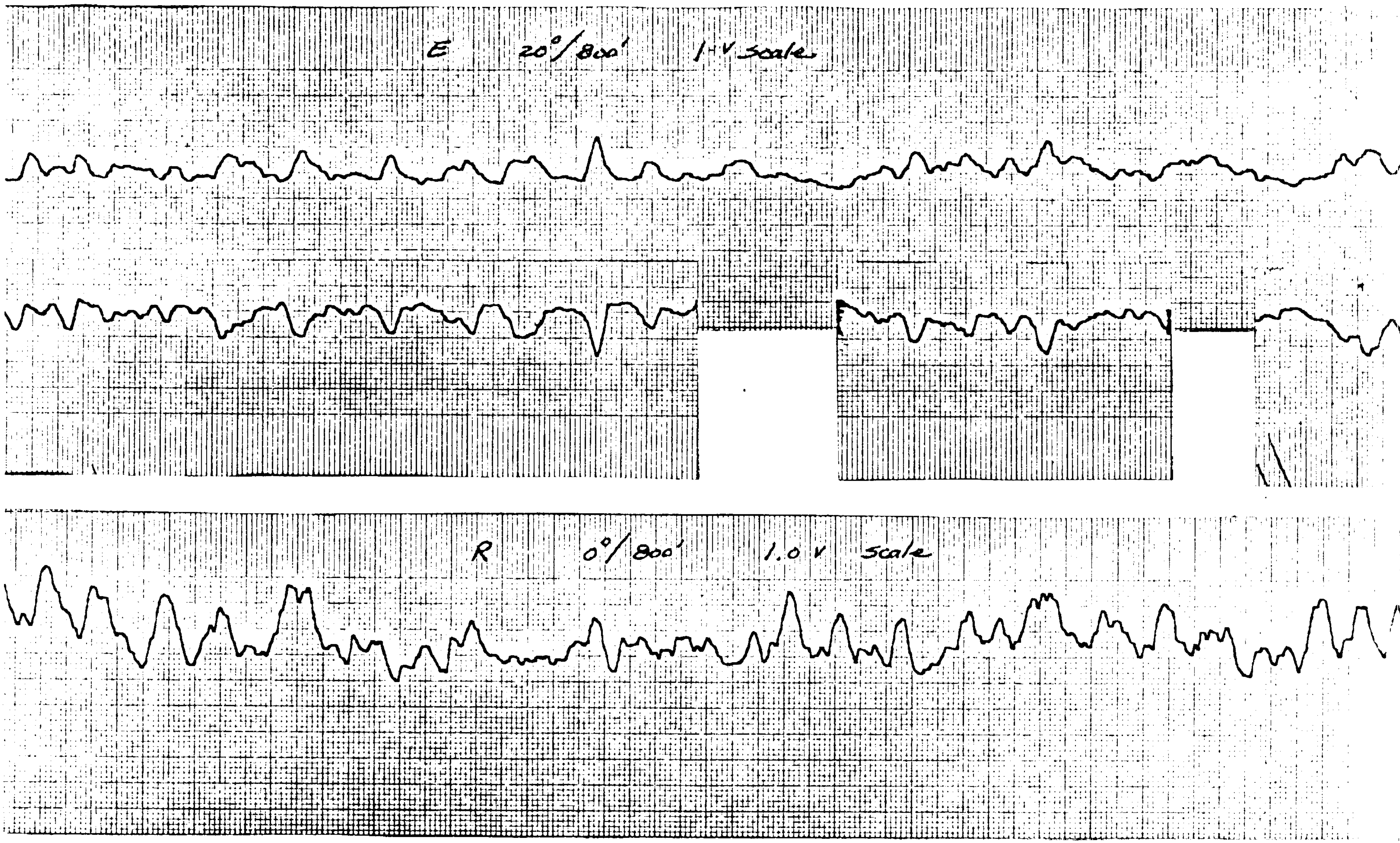

FIG. A-28 AMPLITUDE DETECTOR OUTPUT OF SIMULATED RETURN FOR HUMMOCKS - WSMR
(Sheet 7 of 9)

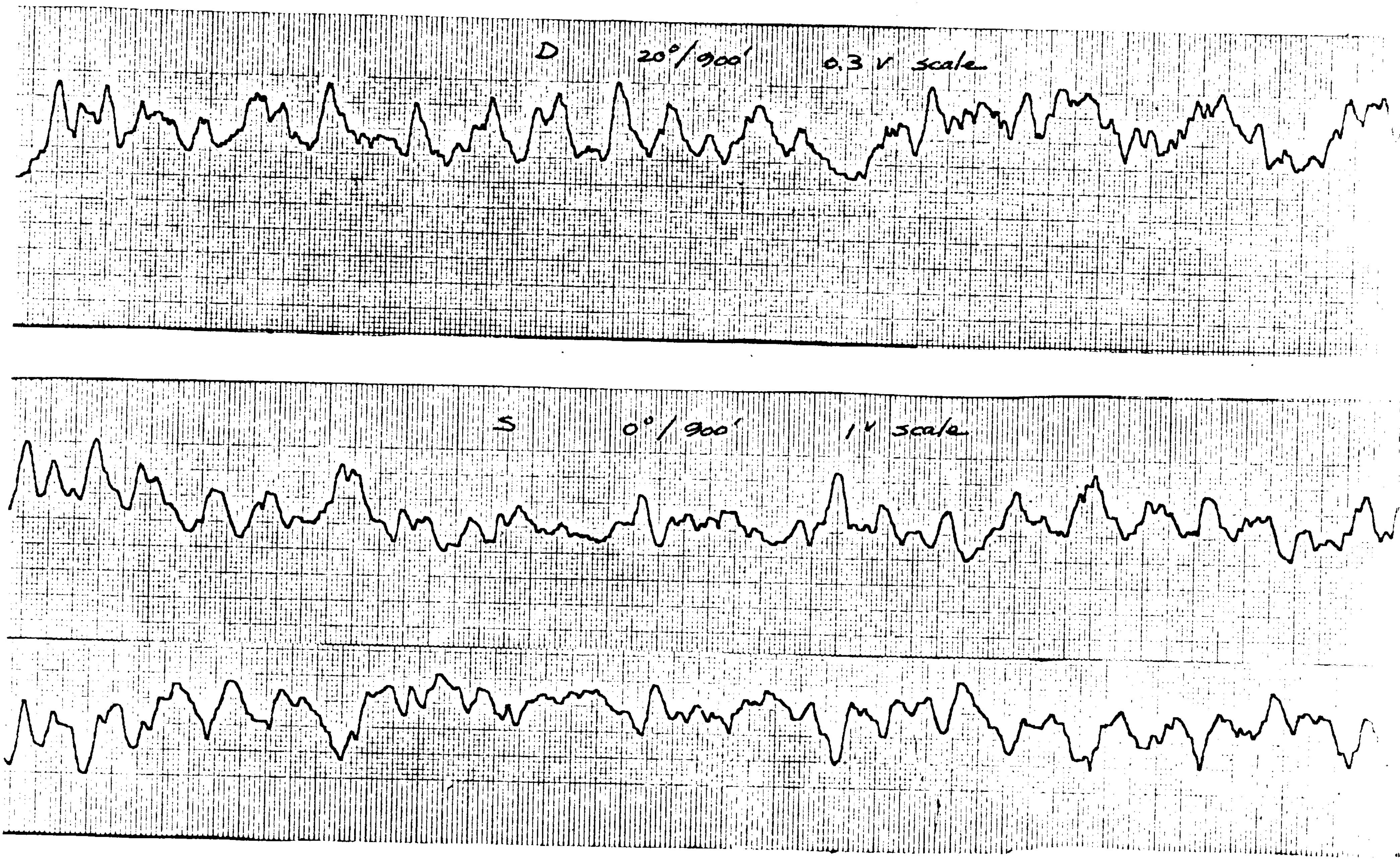

FIG. A-29 AMPLITUDE DETECTOR OUTPUT OF SIMULATED RETURN FOR HUMMOCKS - WSMR
(Sheet 8 of 9)

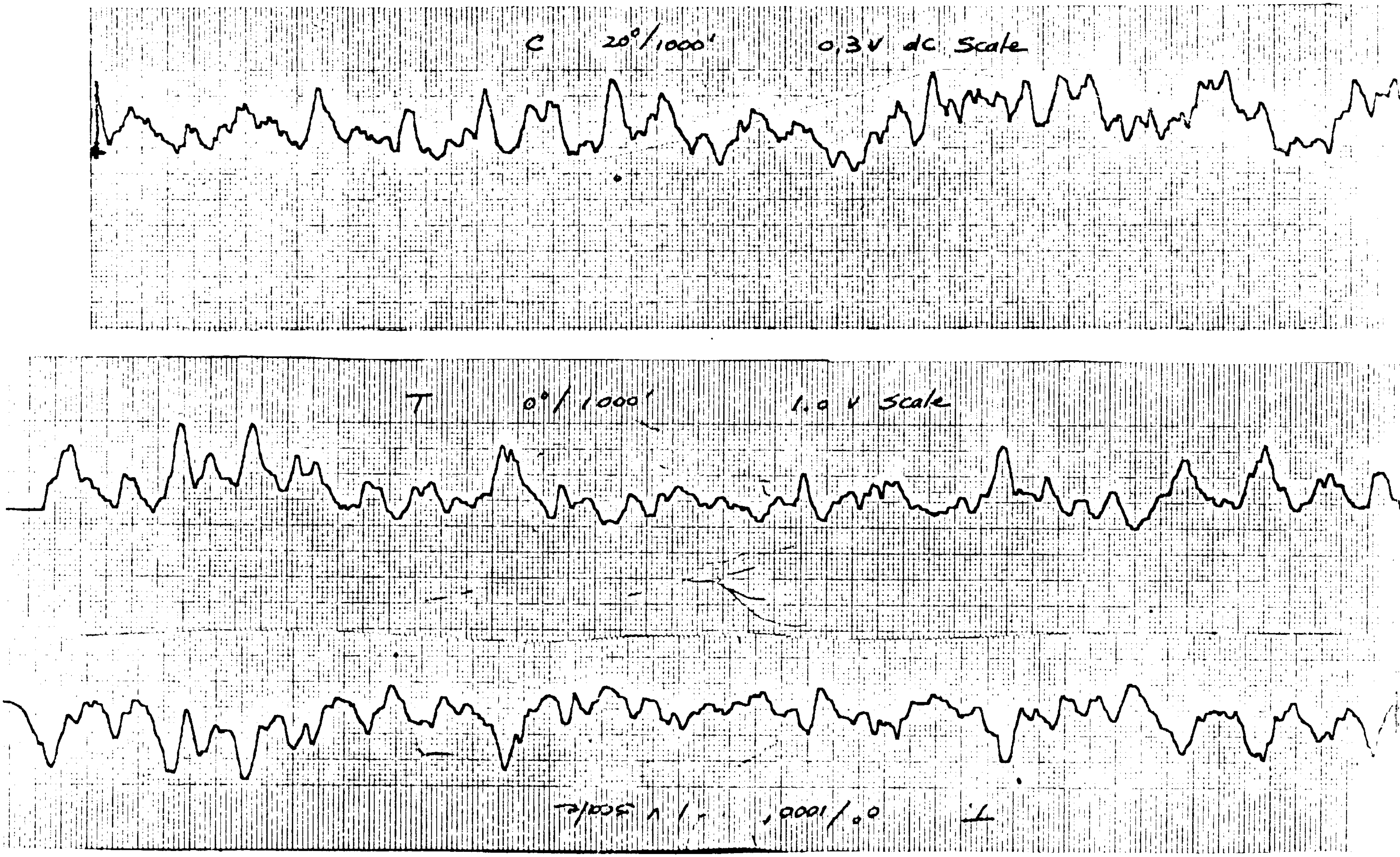

FIG. A-30 AMPLITUDE DETECTOR OUTPUT OF SIMULATED RETURN FOR HUMMOCKS - WSMR
(Sheet 9 of 9)

TABLE A-4

LIST OF MAGNETIC TAPES OF DATA TRANSMITTED TO NASA MANNED SPACECRAFT CENTER ON LUNAR MODEL AND HUMMOCKS (WSMR) MODEL

DATE	TAPE #/Rn#	TARGET	Y(in)	V (dc)	(degrees)	REMARKS**
1/27/68	8/1	P-II-A	42 15/16	22.3	0	1 V.
	8/2		60 2/16	22.3	0	1 V.
	8/3		77 10/16	22.3	0	1 V.
	8/4		95 7/16	22.3	0	1 V.
	8/5		42 15/16	22.3	5	1 V
	8/6		42 15/16	22.3	10	1 V.
	8/7		60 2/16	22.3	10	1 V.
	8/8		77 10/16	22.3	10	1 V.
	8/9		95 7/16	22.3	10	.3
	8/10		42 15/16	22.3	15	.3
	9/11		42 15/16	22.3	20	.3
	9/12		60 2/16	22.3	20	.3
	9/13		77 10/16	22.3	20	.3
	9/14		95 7/16	22.3	20	.3
	9/15		42 15/16	22.3	25	.3
	9/16		42 15/16	22.3	30	.3
	9/17		60 2/16	22.3	30	.3
	9/18		77 10/16	22.3	30	.1
	9/19		95 7/16	22.3	30	.1
	10/20		40 7/16	22.3	35	.1
	10/21		40 7/16	22.3	40	.1
	10/22		60 2/16	22.3	40	.1
	10/23		77 10/16	22.3	40	.1
	10/24		95 7/16	22.3	40	.1
	10/25		40 7/16	22.3	45	.1

11

TABLE A-4 (CONT'D)

DATE	TAPE #/Rn#	TARGET	Y(in)	V (dc)	(degrees)	REMARKS** (2)
2/10/68	12/1 cal	Al. [illegible] Plate	42 15/16		0	.3
	12/2 cal		60 2/16		0	.3
	12/3 cal		77 10/16		0	.1
	12/4 cal		95 7/16		0	.1
2/11/68	13/1	P-II-8	95 7/16	23	0	.1
	13/2		77 10/16	23	0	.1
	13/3		60 2/16	23	0	.1
	13/4		40 7/16	23	0	.3
	13/5		40 7/16	23	5	.3
	13/6		40 7/16	23	10	1.0
	13/7		60 2/16	23	10	1.0
	13/8		77 10/16	23	10	.3
	13/9		40 7/16	23	10	.3
	13/10		40 7/16	23	15	1.0
2/11/68	14/11		40 7/16	23	20	1.0
	14/12		60 2/16	23	20	.3
	14/13		77 10/16	23	20	.3
	14/14		95 7/16	23	20	.1
	14/15		40 7/16	23	25	1.0
	14/16		40 7/16	23	30	.3
	14/17		60 2/16	23	30	.3
	14/18		77 10/16	23	30	.1
	14/19		95 7/16	23	30	.1
	14/20		40 7/16	23	35	.3
	14/21		40 7/16	23	40	.3
	15/22		60 2/16	23	40	.3
	15/23		77 10/16	23	40	.1
	15/24		95 7/16	23	40	.1
	15/25		42 15/16	23	45	1.0

TABLE A-4 (CONT'D)

DATE	TAPE #/Rn#	TARGET	Y(in)	V (dc)	Degrees	REMARKS** (3)
	15/26		[illegible]/16	23	50	.1
	15/27		60 2/16	23	50	.1
	15/28		77 10/16	23	50	.03
	15/29		95 7/16	23	50	.03
.2/68	16/A	White Sands	38 6/16	38	20	3.0
	16/B		38 6/16	43.2	20	1.0
	16/C		24 6/16	43.2	20	.3
	16/D		21.6	43.2	20	.3
	16/E		19.2	43.2	20	.3
	16/F		16.8	43.2	20	.3
	16/G-1		14.4	43.2	20	1.0
	16/G-2		12.0	43.2	20	1.0
	16/H		9.6	43.2	20	1.0
	16/I		7.2	43.2	20	1.0
	16/J		4.8	43.2	20	1.0/.3
	16/K		2.4	43.2	20	not pos.
	16/L		2.4	38.0	0	not pos.
	16/M		4.8	38.0	0	1.0
	16/N		7.2	38.0	0	3.0
	16/0-1		9.6	38.0	0	3.0
	16/0-2		12.0	38.0	0	3.0
	16/P		14.4	38.0	0	3.0
	16/Q		16.8	38.0	0	3.0
	16/R		19.2	38.0	0	1.0
	16/S		21.6	38.0	0	1.0

TABLE A-4 (CONT'D)

ATE	TAPE #/RUN #	TARGET	Y(IN)	V (DC)	DEGREES	REMARKS**
	16/T		24.0	38	0	[illegible]
3/68	17/cal	Flat Plate				
	17/1	White Sands	12.0	38	0	3.0
	17/2		12.0	43.3		1.0
	17/3		12.0	Static	0	10.0
6/68	18/1		2.4	38	0	
	18/2		2.4	38	0	
	18/3		4.8	38	0	
	18/4		24.0		0	
	18/5		24.0	38	20	
	18/6		8.4	38	20	
	18/7		6.1	38	20	

MARKS: These readings correspond to the scale used in the HP-Voltmeter.